

AperTO - Archivio Istituzionale Open Access dell'Università di Torino

Architecture of the Distal Piedmont-Ligurian Rifted Margin in NW Italy: Hints for a Flip of the Rift System Polarity

This is the author's manuscript

Original Citation:

Availability:

This version is available <http://hdl.handle.net/2318/1662001> since 2018-09-06T11:07:13Z

Published version:

DOI:10.1002/2017TC004561

Terms of use:

Open Access

Anyone can freely access the full text of works made available as "Open Access". Works made available under a Creative Commons license can be used according to the terms and conditions of said license. Use of all other works requires consent of the right holder (author or publisher) if not exempted from copyright protection by the applicable law.

(Article begins on next page)

1 **Architecture of the distal Piedmont-Ligurian rifted margin in NW-Italy:**
2 **hints for a flip of the rift system polarity**

3
4 Alessandro Decarlis^{1,2}, Marco Beltrando^{1†} Gianreto Manatschal², Simona Ferrando¹ & Rodolfo
5 Carosi¹

6
7 ¹Dipartimento di Scienze della Terra Università degli Studi di Torino, Via Valperga Caluso, 35, 10125 Torino (I),
8 aledec@tin.it

9 ²EOST/IPGS Université de Strasbourg/CNRS, Rue Blessig, 1, F-67084 Strasbourg Cedex (F)
10

11 **Keywords:** Rift architecture of fossil Alpine margins, upper plate of magma-poor rifted margin, flip in rift
12 asymmetry

13
14 **Abstract**

15
16 The Alpine Tethys rifted margins were generated by a Mesozoic polyphase magma-poor
17 rifting leading to the opening of the Piedmont-Ligurian “Ocean”. This latter developed
18 through different phases of rifting that terminated with the exhumation of sub-continental
19 mantle along an extensional detachment system. At the onset of simple shear detachment
20 faulting, two margin-types were generated: an upper and a lower plate corresponding to the
21 hanging-wall and footwall of the final detachment system, respectively. The two margin
22 architectures were markedly different and characterized by a specific asymmetry. In this
23 study the detailed analysis of the Adriatic margin, exposed in the Serie dei Laghi, Ivrea-
24 Verbano and Canavese Zone, enabled to recognize the diagnostic elements of an upper plate
25 rifted margin. This thesis contrasts with the classic interpretation of the Southalpine units,
26 previously compared with the adjacent fossil margin preserved in the Austroalpine nappes
27 and considered as part of a lower plate. The proposed scenario suggests the segmentation
28 and flip of the Alpine rifting system along strike, and the passage from a lower to an upper
29 plate. Following this interpretation, the European and Southern Adria margins are coevally
30 developed upper plate margins, respectively resting NE and SW of a major transform zone
31 that accommodates a flip in the polarity of the rift system. This new explanation has

32 important implications for the study of the pre-Alpine rift-related structures, for the
33 comprehension of their role during the reactivation of the margin and for the
34 palaeogeographic evolution of the Alpine orogen.

35 **Keywords:** Southalpine domain, Briançonnais domain, Magma-poor rifted margins, Rift
36 flip, Palaeogeographic reconstruction of the Alps.

37

38 **1 Introduction**

39 Remnants of the fossil rifted-margins preserved in the Alps show evidence for a Mesozoic
40 polyphase magma-poor rift evolution [e.g. *Gaetani, 2010; De Graciansky et al., 2011*] that
41 shaped the complex boundary among Africa/Gondwana-derived microplates and Europe
42 [e.g. *Handy et al., 2010; Stampfli et al., 2002*](Fig 1C). These margins formed as a
43 consequence of hyperextension and exhumation of sub-continental mantle along extensional
44 detachment faults, culminating in the opening of the Piedmont-Ligurian basin (Alpine
45 Tethys Ocean Auct.) during late Middle Jurassic [e.g. *Decandia and Elter, 1969; Bezzi and*
46 *Piccardo, 1971; Lemoine et al., 1987; Froitzheim and Manatschal, 1996; Mohn et al.,*
47 *2012*]. The well-preserved Alpine stratigraphic record and its link to extensional rift
48 structures have been widely investigated and compared with seismic images of modern
49 analogues (i.e. Iberia-Newfoundland margins) [e.g. *Manatschal & Bernoulli, 1999*]. In the
50 past few years a conceptual framework for magma-poor margins, which includes a specific
51 nomenclature, has been developed [*Sutra et al., 2013; Tugend et al., 2014; Hauptert et al.,*
52 *2016*]. It accounts for field- and seismic-scale observations made in the Alpine-Pyrenean
53 fossil margins and in the present-day Atlantic and east India magma-poor rifted margins. In
54 this study, after a short review on the Alpine Tethys margins, we apply these new concepts
55 and terminology to the Southern Adria sector exposed in NW Italy. The main goal is to
56 investigate the Jurassic syn-rift sedimentary record and the crustal structures preserved in

57 the Southalpine units to identify the rifting geometry in terms of upper and lower plate [for
58 definitions see: *Hauptert et al.*, 2016]. Results will be used to decipher the general rift
59 architecture and segmentation in the Alpine Tethys system and to discuss the related plate
60 kinematic implications.

61

62 **2 Review on the Alpine Tethys rifted margins**

63 2.1 Geological setting

64 Remnants of the distal Jurassic rifted margins were stacked during Late Cretaceous to
65 Eocene time, forming the present day internal parts of the Central Alps [e.g. *De Graciansky*
66 *et al.*, 2011; *Pfiffner*, 2014]. Margin-derived units rest on either side of the major ophiolite
67 belt (Piedmont-Ligurian units, Fig 1B)[e.g. *Schmid et al.*, 2004; *De Graciansky et al.*, 2011;
68 *Pfiffner*, 2014]. The northwestern rifted margin, formerly belonging to the European plate, is
69 preserved in the Helvetic-Dauphinois-Provençal units (proximal margin, Fig. 1) and in the
70 Briançonnais and Prepiedmont units (distal margin, Fig. 1). Its southeastern counterpart is
71 preserved in the Austroalpine and Southalpine units. Remnants preserved in the
72 Austroalpine units are considered to be derived from the northern segment of the Adria
73 microplate [*Handy et al.*, 2010 cum ref.]. This margin has been interpreted as a conjugate of
74 the European one and is at present separated from the southern segment of Adria, which
75 remnants constitute the Southalpine units, by a major fault zone dividing the south-vergent
76 and almost non-metamorphic part of the chain to the south from a more complex domain to
77 the north [e.g. *Schmid et al.*, 1989] (Fig. 1B). The Southalpine units, object of the present
78 study, belong to the Southern Adria microplate and preserve remnants for both the proximal
79 and distal parts of the former rifted margin [e.g. *Bernoulli*, 1964; *Elter et al.*, 1966; *Sturani*,
80 1973; *Kalin & Trumphy*, 1977; *Berra et al.*, 2009].

81

82 2.2 The concept of hyperextended margins applied to the Alps

83 The Jurassic Alpine Tethys rifted margins were shaped by two discrete extensional phases
84 [Froitzheim and Manatschal, 1996; Berra et al., 2009; Decarlis et al., 2015] that lead to a
85 localization of the deformation from the proximal margin (1st phase: Hettangian-
86 Sinemurian) towards the distal margin (2nd phase: Pliensbachian to Callovian/Bajocian).
87 During this second phase the crust was severely thinned and the subcontinental mantle was
88 exhumed at the seafloor. The geological record of rifting in the Alpine domain has been
89 compared to the evolution of the seismically imaged and drilled Iberia-Newfoundland
90 margins that are considered as the archetypes of upper and lower plate magma-poor rifted
91 margins [e.g. Manatschal and Bernoulli, 1999; Manatschal, 2004; Hauptert et al., 2016].
92 These comparative studies led to the introduction of a conceptual model that may explain
93 the evolution of magma-poor rifted margins [Lavier and Manatschal, 2006]. The model
94 considers three phases of extension: an initial “*stretching phase*” (Fig. 2A/B) that is mainly
95 accommodated in the upper crust by the formation of wide, distributed half-graben systems;
96 a “*thinning phase*” (Fig. 2B/C), leading to the formation of a hyperextended crustal sector
97 (Fig. 3A) bounded by necking zones [see Mohn et al., 2012] that separate the future distal
98 margin from the tectonically inactive proximal margin [definitions in: Sutra et al., 2013;
99 Tugend et al., 2014]; an “*exhumation phase*” related to the exhumation of subcontinental
100 mantle rocks at the seafloor (Fig. 2C-D).

101 For the present study it is important to note that after major crustal thinning, when the
102 residual crust does not contain anymore ductile levels, the rift system becomes asymmetric.
103 Major in-sequence detachment faults split the crust into an upper plate (the hanging wall of
104 the detachment) and a lower plate, formed by the exhumed footwall of the detachment
105 system (Fig. 2C). At this stage, the keystone formed during necking [“H-block” in Lavier
106 and Manatschal, 2006] is laterally delaminated, leading to the formation of extensional

107 allochthons lying on the lower plate. The residual, not delaminated part of the H-block
108 forms the residual H-block ($H_{(r)}$; Fig. 2C) that is the diagnostic feature of an upper plate
109 rifted margin.

110 In the example of the Alpine Tethys margins, the initial stretching phase took place during
111 Hettangian/Sinemurian times [Froitzheim and Manatschal, 1996; Berra et al., 2009;
112 Decarlis et al., 2015], the necking occurred during Pliensbachian/Toarcian [Mohn et al.,
113 2012; Decarlis et al., 2015] and was followed by mantle exhumation and onset of
114 emplacement of Mid Ocean Ridge basalts during Callovian/Bathonian time [e.g. De
115 Graciansky et al., 2011, cum ref.]. Decarlis et al. [2015, and references therein] proposed
116 that the Briançonnais units (distal European margin) forms an upper plate margin and the
117 Lower Austroalpine units (distal Northern Adria margin) the lower plate margin (Fig 1C-D).
118 This interpretation was based on both the analysis of the tectono-stratigraphic record and the
119 recognition of primary rift structures that escaped most of the orogenic overprint in the distal
120 margin [cfr: Mohn et al., 2012; Masini et al., 2013; Decarlis et al., 2015; Hauptert et al.,
121 2016]. The split and left-lateral shift of the two margins has been attributed to the late
122 transpressive evolution of the chain [Decarlis et al., 2015].

123 The fossil rifted margin preserved in the Southern Alps has been analyzed in detail by
124 several authors and has been interpreted as a proximal margin [e.g. Bertotti et al., 1993;
125 Masini et al., 2013], with the exception [Elter et al., 1966; Sturani, 1973] of the
126 westernmost area (Cusio-Biellese zone) that rested in the distal domain [see: Beltrando et
127 al., 2015a; Berra et al., 2009]. Ferrando et al. [2004] analyzed the Canavese Zone and
128 proposed a close similarity with the Lower Austroalpine units exposed in Grisons (SE
129 Switzerland). These authors proposed that the distal Southern Adria margin (i.e. the
130 Canavese Zone) formed as a lower plate margin, too (cfr Fig. 1D).

131

132 3 Polarity of final rifting: geometry and terminology

133 *Hauptert et al.* [2016] introduced, based on previous studies of *Sutra et al.* [2013] and
134 *Tugend et al.* [2014], a specific nomenclature for upper plate magma-poor rifted margins
135 (Fig.2-3A). This nomenclature is of particular relevance for the aim of this paper as it
136 introduces simple morpho-tectonic elements (terraces and ramps) that can be used on
137 seismic sections to recognize the polarity of a rift/detachment system, and therefore, to
138 define upper and lower plate margins. *Hauptert et al.* [2016] introduced “terraces” (T1, T2
139 and T3; Fig. 2) as characteristic features of upper plate margins and discussed them using
140 both fossil (e.g. European-Briançonnais margins of the Alpine Tethys) and present-day
141 examples (East India and Newfoundland margins). Terraces are separated by “ramps” (R1,
142 R2), that correspond to major fault systems formed during the thinning and exhumation
143 phases.

144 In detail, **T1** corresponds to the proximal margin, resting on non-extended or slightly
145 stretched continental crust (30±5 km-thick; Fig. 3A). Wide, fault-bounded half-graben
146 basins hosting thick syn-tectonic successions [cfr. STS1: Syn Tectonic Sequence of *Decarlis*
147 *et al.*, 2015] (Fig. 3B; type 1 basins in Fig. 3D) are the key-features of this domain. The
148 bounding faults of these basins typically sole out into a *decollement* level in the middle crust
149 [see *Bertotti et al.*, 1991; 1993]. Since T1 became inactive when deformation focused in the
150 future distal margin, post-tectonic sediments draped the half-grabens. Thus, the syn-tectonic
151 sequence in the T1 domain predates, by definition, the necking stage and overlies pre-rift
152 successions or upper crust basement only (rift-related exhumation faults do not occur in the
153 T1 domain).

154 The T1 domain is limited oceanwards by a crustal-scale fault system that developed during
155 the thinning phase, forming a morphologic ramp [referred to as **R1** by *Hauptert et al.*, 2016].
156 This zone corresponds to the “necking zone” (see ϕ faults in Fig 3B-C) [*Mohn et al.*, 2012].

157 Sedimentary rocks accumulated during the early development of R1, may account for
158 relatively shallow depositional environments, but they may also be characterized by peculiar
159 features. In fact, differently from half-graben master faults in the T1 domain, the necking
160 fault system forms simultaneously with conjugate fault systems in the lower crust [“coupled
161 domain”: see *Sutra et al.*, 2013]. As a consequence, these faults may allow the advection of
162 deep-seated fluids and they are linked to thermal anomalies and to rapid exhumation of mid-
163 crustal rocks (e.g. heating-cooling cycles) [*Beltrando et al.*, 2015a]. In a rift system, R1
164 marks the boundary between the proximal and the distal margin.

165 The most peculiar feature of upper plate margins is the occurrence of a residual “H-block”
166 [e.g. *Lavier and Manatschal*, 1996], that is up to 50-80 km wide [*Chenin et al.*, 2017] and
167 15-20 km thick. The top of this block is referred to as **T2** [*Hauptert et al.*, 2016]. In the T2
168 terrace, the pre-rift section is only affected by minor brittle high-angle normal faults and the
169 basement is made of upper crust. The syn-rift succession is reduced due to the syn-rift uplift
170 that may generate emersion (see Fig. 3D, type 2 basins).

171 Oceanwards, the T2 is limited by a big morphologic ramp (**R2**), formed by a major normal
172 fault system (φ fault in Fig. 3) accommodating the bathymetric transition to the T3 domain.
173 Along the R2 escarpment, upper crustal rocks (and potentially also remnants of mid-crustal
174 rocks) are exposed. Faulting produces a diffused source for detritic sediments that are
175 collected in new fault-bounded, open-flank basins (Fig. 3C; type 3-4 basins in Fig. 3D) and
176 constitute the typical sedimentary product associated to the thinning phase (syn-tectonic
177 sequence 2: STS2) [*Decarlis et al.*, 2015]. Along R2, the continental crust is split in several
178 tilted blocks, progressively reducing in thickness while approaching the exhumation area
179 (Fig. 3C). The **T3** consists of blocks of pre- and early syn-rift that overlie exhumed lower
180 crust or mantle rocks [see *Masini et al.*, 2011; *Decarlis et al.*, 2015].

181 *Hauptert et al.* [2016] proposed that the remnants of the European Tethys margin exposed in
182 the Western Alps record key structures of an upper plate system. In this example, the T1
183 corresponds to the Dauphinois units exposed today in the external parts of the Western Alps
184 (Fig. 1D). The rift structures in this domain formed during the stretching phase (Hettangian-
185 Sinemurian). The T2 is best preserved in the Briançonnais units (Fig. 1D), that experienced
186 a pronounced uplift during the thinning phase of the Alpine rifting (Pliensbachian-Toarcian)
187 leading to a deep erosion of the substratum that generated a characteristic stratigraphic gap.
188 T3 corresponds to the Prepiedmont and Piedmont units (Fig. 1D), characterized by a
189 complete stratigraphic succession and by a clastic infill during the thinning phase [see: STS2
190 in *Decarlis et al.*, 2015]. It is important to note that in the Austroalpine units of Grisons,
191 considered to be the conjugate margin of the above-mentioned upper plate section [*Decarlis*
192 *et al.*, 2015], the T2 domain does not exist and the T3 is directly passing to the proximal
193 margin (T1: Middle and Upper Austroalpine units; Fig. 1D).

194

195 **4 Southern Adriatic margin**

196 Most of the successions of the Southalpine units contain evidence for a thick stratigraphic
197 record (Fig 4) deposited on basins formed on top of 30±5 km thick continental crust
198 [*Bertotti et al.*, 1991, 1993; *Turrini et al.*, 2014]. During Early Jurassic, half-graben
199 structures developed [e.g. Generoso basin: *Bernoulli*, 1964] and hosted thick syn-tectonic
200 carbonate sequences (Moltrasio and Domaro lms, Medolo group: Hettangian/Sinemurian)
201 [*Berra et al.*, 2009] followed by a suite of pelagic carbonate rocks (Rosso Ammonitico,
202 Concesio Fm: Pliensbachian/Toarcian) [*Berra et al.*, 2009] that draped the topography and
203 marked the passage to a local tectonic quiescence. This area can be therefore interpreted as a
204 typical proximal margin [see *Masini et al.*, 2013].

205 Portions of the distal Southern Adriatic margin crop out in the westernmost sector of the
206 Southalpine units [e.g. *Beltrando et al.*, 2015a] in two different sectors that are here
207 separately described: the Serie dei Laghi-Ivrea Verbano Zone and the Canavese Zone (Fig
208 4).

209

210 4.1 Serie dei Laghi – Ivrea-Verbano zone: basement

211 The Southalpine basement in northwestern Italy is mostly made up of igneous and
212 metamorphic rocks cropping out west of the Southalpine thrusts (Fig. 4) [*Pfiffner*, 2016].

213 Upper crustal rocks (Serie dei Laghi) [*Boriani and Giobbi*, 2004] and middle-to-lower
214 crustal rocks (Ivrea-Verbano zone) [e.g. *Siegesmund et al.*, 2008 *cum ref.*] are exposed at
215 present at the surface as a result of an extensive regional tilting that affected the area during
216 the Alpine orogenic cycle [*Schmid et al.*, 1987].

217 The basement of the Serie dei Laghi is composed of a complex association of Palaeozoic
218 meta-arenites, amphibolites with relicts of gabbros, ultramafites and paragneisses, meta-
219 pelites and ortogneisses [*Boriani and Giobbi*, 2004]. These rocks were intruded by
220 voluminous granitoid bodies during Early Permian [*Boriani et al.*, 1988] and represent a
221 portion of the upper crust since Paleozoic times.

222 The Ivrea-Verbano Zone is a pre-Jurassic middle/lower crustal unit that is composed of
223 high-temperature amphibolite to granulite facies rocks. It includes kinzigites that represent
224 former metasedimentary to metavolcanic successions [*Novarese*, 1929], partly intruded by a
225 Permian large mafic complex [*Rivalenti et al.*, 1981; *Voshage et al.*, 1990; *Pfiffner*, 2014
226 and *ref. therein*]. West of the mafic complex, isolated bodies of subcontinental mantle rocks
227 occur (Fig. 4: Balmuccia, Finero, Baldissero) [*Rivalenti et al.* 1981; *Garutti et al.* 1979;
228 *Shervais*, 1979; *Voshage et al.*, 1988; *Hartmann & Wedepohl*, 1993]. Lowermost levels of
229 the Ivrea-Verbano Zone are separated from the Sesia-Lanzo Zone by the fault system of the

230 Insubric Line that reached anchizone to low-greenschist facies conditions. Important
231 structures, relevant for the interpretation of the Jurassic Adriatic margin, occur near the
232 stratigraphic top of the Ivrea-Verbano Zone. The Cossato-Mergozzo Brissago Line is a NE-
233 SW striking fault zone that marks the contact between the Serie dei Laghi and the Ivrea-
234 Verbano Zone (CMB: Fig. 2) [Handy, 1987]. It consists of high-temperature mylonites
235 associated with migmatites and dykes related to Early Permian extension (Ar/Ar age: 271 ± 1
236 Ma) [Boriani and Villa, 1997] (Ru/Sr; 275 ± 8 Ma) [Pinarelli et al., 1988]. The Cossato-
237 Mergozzo-Brissago Line is overprinted by a younger fault system, the Pogallo Line (PL:
238 Fig. 2) [Handy, 1987]. The latter is a ductile shear zone, characterized by subvertical
239 foliation with SW-NE strike and NE plunging stretching lineations with a left-lateral sense
240 of shear. It consists of mylonites developed under amphibolite to greenschist facies
241 conditions, striking NE-SW in the northern branch and roughly N-S toward the south (Fig.
242 4). The age of the Pogallo Line has been constrained to 200-180 Ma by Zingg et al. [1990].
243 The late stage of faulting occurred under lower greenschist conditions and close to the
244 brittle-ductile transition and has been related to Early Jurassic [Zingg, 1990 cum ref.]. It has
245 been interpreted as an east dipping, mid-crustal extensional listric fault that accommodated
246 extension during Jurassic rifting [Handy et al., 1999].

247

248 4.2 Serie dei Laghi: sedimentary cover

249 Toward the south, the Serie dei Laghi is crossed by an E-W fault system with a right lateral
250 and a vertical component (Cremonina Line: CL: Fig 4) [Boriani and Sacchi, 1973]. As a
251 result of this latter structure, the sedimentary cover of the Serie dei Laghi is only preserved
252 south of the Cremonina Line. Scarce remnants of Mesozoic sedimentary rocks actually crop
253 out in between Lago Maggiore and Sostegno (Fig 4), but most of them are buried further to
254 the south under the Po plain alluvials and are only imaged by seismic profiles [Fantoni et

255 *al.*, 2003; *Pfiffner*, 2014, 2016]. The Mesozoic sedimentary record of the western
256 Southalpine is extremely lacunous if compared to the successions of the Lombardian basin.
257 This marked difference has been described in the literature [*Berra et al.*, 2009; *Fantoni et*
258 *al.*, 2003; *Beltrando et al.*, 2015a]. The syn-rift sequence is visible only at selected locations.
259 A brief description of the key-stratigraphic features of the most relevant outcrops based on
260 personal observations and on the cited literature is described below (Fig. 5).

261 - *Arona* (Fig. 5; Fig. 6a): a thin succession of Early to Middle Triassic sandstones overlies
262 Permian volcanic rocks. Sandstones are overlain by Middle Triassic Dolostones (San
263 Salvatore Dolostones) [*Zanin Buri*, 1965]. A widespread monogenic breccia body can be
264 observed draping the dolostones at the top and laterally. It is almost exclusively composed
265 of angular clasts of Triassic dolostones but some rare fragments of reddish pelites with small
266 rounded dolomite clasts can be found. Reddish pelite clasts were probably eroded from
267 paleokarsts similar to those found in the Fenera-Sostegno area (Fig. 6e) and that are
268 considered Jurassic [*Fantoni et al.*, 2003; *Berra et al.*, 2009]. In our interpretation, the
269 Arona breccia was generated by a rock-fall depositional process during Early Jurassic
270 rifting, testifying the dismantling of the Triassic sediments in a subaerial environment.

271 - *Invorio* (Fig. 5; Fig. 6b): in this location clast-supported polygenic breccia (“*Invorio*
272 *Breccia*”) [*Casati*, 1978] was likely directly deposited on the Serie dei Laghi basement.
273 Breccias correspond to local accumulations with poor evidence for bedding or relevant
274 sedimentary structures. It is composed of centimetric to decimetric clasts of Serie dei Laghi
275 basement, Permian volcanic fragments and Triassic dolostones.

276 The limited extension of the outcrops and the lack of sharp upper and lower stratigraphic
277 boundaries do not allow to properly correlate the Invorio breccias, nevertheless it has been
278 interpreted as a continental deposit of Jurassic age [*Casati*, 1978].

279 - *Gozzano* (Fig. 5; Fig.6c,d): at this locality a few tens of meters of a Jurassic succession
280 probably laying on the Permian volcanic rocks can be observed [*Montanari*, 1969].
281 However, this boundary is not visible at present. The Jurassic succession is formed by
282 calcarenites, microbreccias and calcilutites with brachiopods, corals and crinoids (here
283 informally named Lithozone "A") overlain by nodular limestones and calcarenites with
284 ammonoids and molluscs (Lithozone "B"). The whole succession was affected by important
285 fluid activity that led to the formation of widespread calcite-dolomite veins. Lithozone "A"
286 has been ascribed to the Upper Sinemurian-Lower Pliensbachian (?), Lithozone "B" to the
287 Upper Pliensbachian on the base of a rich fossil fauna [*Sacchi Vialli and Cantaluppi*, 1967;
288 *Montanari*, 1969]. *Montanari* [1969] reported that Upper Pliensbachian sedimentary rocks
289 were filled with neptunian dikes that opened inside the lithozone "A" and described an
290 angular unconformity between the two lithozone suggesting that a tectonic pulse occurred
291 during Late Early Jurassic. The Jurassic succession at Gozzano has been interpreted as
292 deposited on top of a submarine high [*Berra et al.*, 2009].

293 - *Monte Fenera and Sostegno* (Fig. 5): at these localities more complete Mesozoic
294 successions are preserved. Permian volcanic rocks are overlain by a thin succession of
295 sandstones and conglomerates that predate the deposition of Middle Triassic dolostones
296 [see: *Fantoni et al.*, 2003; *Berra et al.*, 2009]. The top of Ladinian carbonate rocks is
297 characterized by a widespread unconformity, locally accompanied by karstified levels and
298 followed by a thin succession of dolomitic breccias, conglomerates and micro-
299 conglomerates with oxidized reddish matrix both at Fenera and Sostegno (Fig 6e).
300 Sedimentary dykes filled of the same reddish material and of dolomitic breccias can be
301 frequently found (Fig. 6f). The unconformity has been interpreted as a complex surface,
302 probably related to a prolonged erosion and karstification event leading to the deposition of
303 reworked palaeosoils and breccias [*Fantoni et al.*, 2003; *Berra et al.*, 2009].

304 A 50 meter-thick succession of lithic sandstones (San Quirico Sandstone) composed of
305 dolomitic, volcanic and basement-derived grains [Fantoni *et al.*, 2003; Berra *et al.*, 2009]
306 overlays the breccia. The depositional age for these sandstones has been determined by
307 palinomorphs as Pliensbachian-Toarcian [Berra *et al.*, 2009]. Interestingly, (U-Th)/He
308 analysis on zircons in volcanic grains of the sandstone gave comparable absolute cooling
309 ages (171 ± 14 Ma and 177 ± 14 Ma respectively for Fenera and Sostegno) [Beltrando *et al.*,
310 2015a]. These data demonstrate that the process of exhumation, cooling, erosion and
311 sedimentation was very rapid. San Quirico Sandstone is overlain by some hundred of meters
312 of spongolitic limestone of Pliensbachian?-Toarcian age.

313

314 4.3 Canavese Zone

315 The Canavese Zone [Argand, 1909] is a structural unit, about 2 km wide and 40 km long,
316 bounded by two main SW-NE faults: the External Canavese Line (ECL: Fig 4) to the
317 northwest, and the Internal Canavese Line (ICL: Fig. 4) to the southeast [Biino *et al.*, 1988;
318 Biino and Compagnoni, 1989] (Fig 4). The External Canavese Line, or the Canavese Line
319 s.s., is the southwestern branch of the Insubric Line. The Internal Canavese Line is a ductile
320 shear zone producing very low-grade Alpine mylonites separating the Canavese Zone from
321 the granulite-facies rocks of the Ivrea Verbano Zone [Biino *et al.*, 1988; Biino and
322 Compagnoni, 1989]. Upper, middle and lower crustal rocks are present in the Canavese
323 Zone, although their relationships are often not easy to decipher.

324 - The upper crust outcrops near Montalto (Fig. 4A) and is composed of a Palaeozoic
325 association of paragneiss, phyllites, banded albite-epidote-actinolite metabasics and augen-
326 gneiss [Baggio, 1965a; Biino *et al.*, 1988; Biino and Compagnoni, 1989]. The metamorphic
327 suite is locally intruded by Permian plutonic rocks [Biino *et al.*, 1988; Biino and

328 *Compagnoni, 1989*] and is overlain by Permian volcanic rocks similar to those found in the
329 Fenera-Sostegno area.

330 - Mid crustal rocks outcrop near Baldissero (Fig. 4A) and are composed of a
331 heterogeneous assemblage of amphibolite-facies rocks, such as amphibolites, biotite-
332 gneisses \pm garnet, and muscovite-biotite schist with garnet \pm fibrolitic sillimanite [*Baggio,*
333 1965b; *Wozniak, 1977; Borghi et al., 1996; Ferrando et al., 2004*].

334 - Lower crustal rocks outcrop near Baldissero and Levone (Fig. 4A) and are composed
335 of migmatites with transitional contacts to anatectic leucogranite [*Baggio, 1965b; Wozniak,*
336 1977; *Ferrando et al., 2004*]. The lower crustal rocks have never been observed to be
337 intruded by the post-Variscan intrusive rocks. On the contrary, they locally include
338 fragments of mafic granulites similar to those of the Ivrea-Verbano Zone [*Wozniak, 1977;*
339 *Ferrando et al., 2004*].

340 The pre-rift sedimentary succession mainly outcrops near Montalto Dora (Fig. 4). It is
341 formed by conglomerates and sandstones (Permian-Early Triassic in age) followed by
342 Triassic dolostones. The age of the carbonate rocks remains uncertain, due to the lack of
343 fossils, but they have been compared in the literature [*Baggio, 1965a*] to those found at
344 Arona and Fenera-Sostegno and interpreted as Middle Triassic on the basis of the facies and
345 lithologic features. Dolostones are cut by several neptunian dykes and sills filled by a
346 reddish/greenish matrix and by clasts derived from the underlying lithologies [*Biino et al.,*
347 1988; *Biino & Compagnoni, 1989*]. Dolostones are locally overlain by red calcarenites dated
348 as Early Sinemurian by ammonoid occurrence [*Sturani, 1964*]. Breccias can be observed
349 directly laying on the Triassic carbonates. They are formed by dolostones and reddish
350 calcarenite clasts in a reddish or greenish matrix similar to the filling of the neptunian dykes.
351 Syn- to post-rift sedimentary rocks have been reported to directly lie on top of the
352 migmatites in the areas near Baldissero e Levone (Fig. 4) [*Ferrando et al., 2004*]. These

353 successions are characterized by a stratigraphic transition from the cataclastic lower crust to
354 a clast-supported tectono-sedimentary breccia [Manatschal, 1999] (Fig 6g) and finally,
355 toward the top, to a polymictic breccia (clasts of both lower and middle crusts, intrusive and
356 volcanic rocks and phyllonites) [Ferrando et al., 2004; Beltrando et al., 2015b]. A
357 Pliensbachian to Bajocian age has been proposed for the breccia/arkosic-pelitic sequence
358 because of the marked similarity with the syn-rift Saluver Formation of the Austroalpine
359 nappes of the Grisons in SE-Switzerland [Carraro and Sturani, 1972; Ferrando et al.,
360 2004]. In the Levone area (Fig. 4), the tectono-sedimentary breccias are dissected by shear
361 zones associated to a characteristic chromium-rich fault gouge [Beltrando et al. 2015b].
362 Similar fault-rocks have been described in the Lower Austroalpine Err nappe in Grisons
363 along extensional detachment faults [Manatschal, 1999]. These fault-rocks have been shown
364 to result from the alteration by mantle-derived fluids along exhumation faults that penetrated
365 and exhumed the subcontinental mantle to the Jurassic seafloor. This similarity drove
366 Beltrando et al. [2015b] to suggest the same interpretation for the Canavese gouges of the
367 Levone sector, where they crop out close to the large serpentized peridotite body of
368 Pesmonte.

369 Post-rift sedimentary rocks mainly outcrop near Baldissero (Fig. 4) and are made of
370 Radiolarites (Fig. 6h), micritic limestones of the Maiolica formation (Tithonian-Berriasian)
371 [Baggio, 1963] and marly limestones considered to be equivalent to the Palombini Shales
372 [Ferrando et al., 2004]. These sediments, most likely of Early Cretaceous age, represent the
373 youngest sedimentary rocks found in the Canavese Zone.

374 **5 Discussion**

375 **5.1 Interpretation of the architecture of the Southern Adria distal margin**

376 In the following, we apply the classification criteria and diagnostic features used by Tugend
377 et al. [2014] and Hauptert et al. [2016] to characterize the architecture of the Southern Adria

378 margin. The Southalpine successions of the Orobic and Lombardic nappes have been
379 classically ascribed to a proximal margin [*Bertotti et al.*, 1993; *Masini et al.*, 2013 *cum ref.*],
380 or a T1 terrace [*Hauptert et al.*, 2016]. The Canavese Zone was interpreted as an analogue
381 for the Lower Austroalpine Err unit in Grisons [*Ferrando et al.*, 2004], *i.e.* as a part of the
382 lower plate. At present, these sectors are preserved within different tectonic units separated
383 by large-scale structural contacts. The Serie dei Laghi - Ivrea-Verbano Zone basement
384 complex is placed in between these two units and exposes a deep crustal section at the
385 surface due to orogenic tilting. This area assumes a key-role as indicator for the polarity of
386 the rift system. The peculiar stratigraphic record associated to the scarce, starved
387 sedimentary cover of the Serie dei Laghi (Cusio-Biellese zone) led *Berra et al.* [2009] to
388 interpret it as part of the distal margin of Southern Adria.

389 The boundary between the proximal and the most distal margin corresponds, as shown in
390 Fig. 3, to the necking zone, a system of convex-concave faults respectively dissecting the
391 upper-to-middle and the middle-to-lower crust. For the case of the Southern Adria margin,
392 the conjugate necking faults may be located inside the Serie dei Laghi – Ivrea-Verbano Zone
393 and, due to its tilting along a horizontal axis, they must mainly crop out respectively south
394 and north of the Cremosina Line (Fig. 4).

395 -The upper necking fault system (N1: Fig. 7) is located in the easternmost area of the Serie
396 dei Laghi – Ivrea-Verbano zone, south of the Cremosina Line and between the Lago
397 Maggiore and M. Fenera (Fig. 4). Although anthropization and widespread quaternary
398 deposits prevents the exposure of the upper necking fault system in the field, indirect
399 evidences for its occurrence are represented by the “Jurassic faults” dissecting N-S the
400 Permian volcanic rocks and the Serie dei Laghi [*Sbisà*, 2010]. Moreover, this area was
401 exposed at the surface during rifting, as subaerial syn-rift sedimentary rocks directly overlap
402 basement or slice of reduced pre-rift successions (Invorio and Arona). The erosion of the

403 exposed basement formed syn-rift sandstones accumulations to the west (San Quirico
404 Sandstone at M. Fenera and Sostegno). These sandstones preserve evidence for their
405 peculiar heating-cooling history, never found elsewhere in the Southalpine units. U-Th/He
406 analysis on zircons from these sandstones provided ages comparable with those of their
407 deposition (Pliensbachian-Toarcian) [Beltrando *et al.*, 2015a]. This suggests that: (i) source
408 rocks were exhumed and cooled along major crustal faults, (ii) they were rapidly eroded and
409 (iii) sandstones were deposited in shallow water basins. Therefore we interpret Arona and
410 Inverio to lie close or on top of the emerged upper necking fault system (N1: Fig. 7)
411 footwall, whereas Gozzano remained into an isolated but tectonically active submerged
412 environment.

413 -The lower part of the necking system (Fig. 7: N2) is formed by a concave crustal-scale fault
414 that, by definition, intersects the upper system N1 in the Coupling Point (Fig. 3: CP). In a
415 3D view the coupling point becomes a line (see Fig. 7). In this study we propose that the
416 northern part of the Pogallo Fault Zone may correspond to the east dipping lower part of the
417 necking fault system (N2 in Fig. 7). Toward the south, close to the Orta Lake (Fig. 4), the
418 fault possibly reaches the coupling point. This southern segment of the Pogallo Line may
419 thus represent the projection of the coupling point in a map view (*i.e.* a NE dipping coupling
420 line).

421 Thus, north of the Cremosina Line, the Pogallo fault system separates two distinct crustal
422 blocks owing to the distal (to the west) and to the proximal margin (to the east). Their
423 basement rocks preserve evidence for a complex pre-Alpine evolution of the Southalpine
424 units [Boriani *et al.*, 2004], but also for a Jurassic shear and/or tectono-magmatic activity in
425 the Pogallo Fault [Handy, 1999] and in the Ivrea-Verbano Zone [Zanetti *et al.*, 2013].

426 Based on this interpretation, the domain exposed west of the Lago Maggiore corresponds to
427 a R1-T2 [Hauptert *et al.*, 2016], *i.e.* it is in an equivalent position to the Briançonnais domain

428 along the European margin (see Fig. 8). Direct evidence comes from the sedimentary record
429 preserved in Cusio-Biellese zone that is crucial for this interpretation. In fact, sedimentary
430 rocks testify a stage of emersion during rifting with deep erosion and karstification of the
431 substratum (M. Fenera and Sostegno), followed by deposition of shallow water sediments
432 during the thinning phase. Low organic matter maturity data suggest that the sedimentary
433 cover experienced a moderate thermal gradient with temperatures in the sedimentary rocks
434 never exceeding 60-70 °C [Fantoni & Scotti, 2003]. These data place this sector relatively
435 “high” along a hypothetic passive margin profile (i.e. with low burial temperature). In
436 addition, Mesozoic sedimentary basins seismically imaged further south underneath the Po
437 plain [Fantoni *et al.*, 2003] are relatively thin and localized, suggesting that moderate
438 deposition and erosion are not exclusive features of the Serie dei Laghi cover exposed at the
439 surface, but can be extended to the whole sedimentary sequence further to the southwest.

440 Further, but indirect evidence comes from the preserved width of the Serie dei Laghi distal
441 margin, that can be tentatively estimated in the order of 50-60 km. Since during alpine
442 compressional phases this area was only shortened N-S, perpendicular to the strike of the
443 margin, we assume that these 50 to 60 km roughly correspond to the original width of the
444 interpreted Adria T2. A global estimation of T2 compiled from different margins by *Chenin*
445 *et al.* [2017] is in the order between 50-80 km. Moreover, restorations of the Briançonnais
446 domain (also interpreted as a T2) [Hauptert *et al.*, 2015] are in the order of 50-60 km [Mohn
447 *et al.*, 2010 *cum ref.*].

448 More critical is the interpretation of the Canavese Zone that can be described as a complex
449 unit formed by several tectonic elements in which the convergence and orogenic phases of
450 the Alpine cycle probably juxtaposed portions of the R2 (Montalto Dora) and the transition
451 to the T3 (Levone).

452

453 5.2 Palaeogeographic implications

454 The identification of a T2 domain in the distal margin of Southern Adria implies that it has
455 to be interpreted as an upper plate margin during the opening of the Piedmont-Ligurian
456 basin. Thus the tectono-stratigraphic analysis of the rifted margins of the Alps suggests that
457 both the distal European [*Decarlis et al.*, 2015; *Hauptert et al.*, 2016] and distal Southern
458 Adria margins were upper plate systems (Fig. 8). On the contrary, the Northern Adria
459 margin exposed north of the Insubric Line in the Austroalpine nappes and considered to be
460 conjugate to the European margin [*Decarlis et al.*, 2015], was interpreted as a lower plate
461 [*Manatschal*, 2004].

462 If these margins are plotted into a palaeogeographic map of the Alpine realm (Fig. 8), it
463 becomes clear that two conjugate pairs can be identified: one to the north (T1: Provençal,
464 T2: Briançonnais, R2-T3: Pre-Piedmont and Piedmont-Ligurian, destroyed T2: Lower
465 Austroalpine, T1: Upper Austroalpine; see Fig. 8) and one, incomplete, to the south (T1:
466 Southalpine s.s., T2: Serie dei Laghi – Ivrea-Verbano Zone, R2-T3 Canavese zone; Fig. 8)
467 separated by a major tectonic system locally represented by the Insubric Line. Conjugate
468 pairs remnants are thus flipped in the Alpine rift geometry.

469 Such configuration can be compared with those observed in core complex systems [*Lister et*
470 *al.*, 1986], in which the rifting geometry flips across “transfer faults” that accommodate the
471 different dips of contiguous detachment faults. *Lister et al.* [1986] also proposed that the
472 mechanism of detachment faulting is part of the continental extension process and that thus
473 similar geometries are to be expected in passive margins.

474 In fact, along strike variations in the distribution of upper and lower plate systems have been
475 recently observed in seismic profiles of the Western Africa margins of the Atlantic Ocean.
476 In the Angola-Gabon rifted margin upper and lower plates alternate and the change of
477 polarity is accommodated by different type of transfer zones [*Peron-Pinvidic et al.*, 2017].

478 We propose that a similar transfer zone had to be active during Jurassic time along the
479 Palaeo-Insubric Line system (Fig. 8).

480 An important consequence of this interpretation is related to the position of the Corsica-
481 Sardinia block in the proposed palaeogeographic reconstruction (Fig. 8), that deviates from
482 the *Handy et al.* [2010] model. In fact, as Corsica and Sardinia have been usually interpreted
483 as the southern continuation of the Briançonnais realm and display a marked tectono-
484 stratigraphic affinity with this domain [e.g. *Costamagna, 2016 cum ref.*], they can be
485 considered as part of an upper plate system. For this reason they rested toward the north in
486 respect to the suggested transfer fault and in a similar palaeogeographic position to that
487 proposed by *Thierry et al.* (2000a,b). This would place the Sardinia-Corsica-Briançonnais
488 block on the SW edge of the European plate. According to this configuration, the Jurassic
489 palaeo-Insubric transfer zone merged the plate boundary between Europe and Iberia to the
490 NW.

491 After the rifting and drifting phase, the palaeo-Insubric transfer system was then reactivated
492 during the successive stages of the Alpine cycle, accommodating the oblique convergence
493 and the continental collision during Cretaceous and Cenozoic.

494 We also suggest that the Jurassic transfer zone may have superimposed on a pristine major
495 fault system. In fact several studies hypothesized a widespread transcurrent-extensional
496 activity during Late Palaeozoic and Triassic in the Alps [e.g. *Muttoni et al., 2003:*
497 *Southalpine; Doglioni, 1987: Dolomites; Decarlis et al., 2013 cum ref. : Ligurian Alps*].
498 This suggests that major transcurrent discontinuities at an orogen-scale (e.g. the Insubric
499 system) may be inherited from former rift events and can survive and control later orogenic
500 phases. This interpretation may open new interesting questions about the role of rifting-
501 related inheritance during orogenic evolution and may help to better define the kinematic
502 evolution of the strongly debated Alpine palaeogeography.

503

504 7 Conclusion

505 The tectono-stratigraphic setting of the Southern Adria rifted margin preserved in NW Italy
506 suggests that this sector can be interpreted as an upper plate system. The proximal margin
507 [T1 in *Hauptert et al.*, 2016] is preserved in the central-eastern Southalpine units, while
508 distal parts of the former margin crop out in the Serie dei Laghi – Ivrea-Verbano Zone and
509 Canavese Zone, that respectively represent T2 and R2-T3 domains of *Hauptert et al.* [2016].
510 This observation is not in agreement with the classic interpretation of the Alpine rifted
511 margins that account for an NW located upper plate (European plate) and a SE lower plate
512 (Northern and Southern Adria) throughout the whole Alpine rift system. The proposed
513 configuration accounts for two distinct type-sections across the Alpine rifted margins that
514 exhibit a flip of the distal geometry of the Alpine Tethys margins. As reported by *Decarlis*
515 *et al.* [2015], the upper plate along the Europe-Northern Adria margins is located to the NW
516 and corresponds to the Briançonnais Zone. In the studied Southern Adria margin, the upper
517 plate is located to the SE. This setting requires that a major flip occurred along strike of the
518 Piedmont-Ligurian rifting system. The present study proposes that these two sectors are
519 separated by a tectonic system comparable to the “transfer faults” proposed by *Lister et al.*
520 [1986] and observed at present-day margins. This fault zone probably survived the rifting
521 stage and was reactivated during the whole orogenic cycle forming a key crustal-
522 discontinuity that conditioned the large-scale kinematics of the Western Mediterranean and
523 its palaeogeographic evolution since the Mesozoic.

524

525 Acknowledgements

526 We gratefully thank Giancarlo Molli, Adrian Pfiffner and Gideon Rosenbaum for helpful
527 reviews that significantly improve the manuscript. The research was supported by Torino
528 University Grant (Torino_call2014_L1_202; Resp. S.F.) and by MM4 consortium (Margin

529 Modelling Phase 4: Liverpool & Strasbourg University), taking benefits from useful
530 discussions with colleagues from the academic and industrial partners. The data supporting
531 this paper are available within figures 5-7.

532

533 **References**

534 Baggio, P. (1963), Sulla presenza di una serie titonico-cretacea nel Canavese s.s. (Prealpi
535 Piemontesi), *Atti Ist. Veneto Sci. Lett. Arti*, 121, 215–234.

536 Baggio, P. (1965a), Caratteri stratigrafici e strutturali del Canavese s.s. nella zona di
537 Montalto Dora (Ivrea), *Mem. Ist. Geol. Min. Univ. Padova*, 25, 1-25.

538 Baggio, P. (1965b), Geologia della Zona del Canavese nel settore occidentale Levone-
539 Cuorné (Prealpi Piemontesi), *Mem. Acc. Patavina S.M.N.*, 77, 41-72.

540 Beltrando, M., D. F. Stockli, A. Decarlis and G. Manatschal (2015a), A crustal-scale view at
541 rift localization along the fossil Adriatic margin of the Alpine Tethys preserved in NW
542 Italy, *Tectonics*, 34, 1927-1951, doi: 10.1002/2015TC003973.

543 Beltrando, M., R. Compagnoni, S. Ferrando, G. Mohn, G. Frasca, N. Odasso, Z.
544 Vukmanovič and E. Masini (2015b), Crustal thinning and mantle exhumation in the
545 Levone area (Southern Canavese Zone, Western Alps), in A Field Guide Across the
546 Margins of Alpine Tethys, J. Virtual Explor. 48, edited by G. Manatschal et al., *Journ.*
547 *Virtual Explorer*, Pty. Ltd., Clear Range, Australia, doi:10.3809/jvirtex.2013.00326.

548 Bernoulli, D. (1964), Zur geologie des Monte Generoso ein beitrage zur kenntnis der
549 süddalpinen sedimente, *Beitr. Geol. Karte Schweiz*, N.F. 118, Zurich.

550 Berra F. and E. Carminati (2010), Subsidence history from a backstripping analysis of the
551 Permo-Mesozoic succession of the Central Southern Alps (Northern Italy), *Basin*
552 *Research*, 22 (6), 952-975.

553 Berra, F., M. T. Galli, F. Reghellin, S. Torricelli and R. Fantoni (2009), Stratigraphic
554 evolution of the Triassic- Jurassic succession in the Western Southern Alps (Italy): the
555 record of the two-stage rifting on the distal passive margin of Adria, *Basin Research*, 21,
556 335–353.

557 Bertotti, G., V. Picotti and D. Bernoulli (1991) Early Mesozoic extension and Alpine
558 shortening in the western Southern Alps: the geology of the area between Lugano and
559 Menaggio (Lombardy, northern Italy), *Mem. Sci. Geol. Padova*, 43, 17–123.

560 Bertotti, G., V. Picotti, D. Bernoulli and A. Castellarin (1993), From rifting to drifting:
561 tectonic evolution of the South-Alpine upper crust from the Triassic to the Early
562 Cretaceous. *Sed. Geol.*, 86, 53–76.

563 Bezzi, A. and Piccardo, G.B. (1971) Structural features of the Ligurian ophiolites: petrologic
564 evidence for the “oceanic” floor of the Northern Appennine geosyncline: a contribution to
565 the alpine-type gabbro-peridotite associations. *Mem. Soc. Geol. It.*, 10, 55-63.

566 Biino, G., R. Compagnoni and M. Naldi (1988), The Canavese Zone near Ivrea (Western
567 Alps), *Rend. Soc. Geol. It.*, 11, 85-88.

568 Biino, G. and R. Compagnoni (1989), The Canavese Zone between the Serra d’Ivrea and the
569 Dora Baltea River (western Alps), *Eclogae Geol. Helv.*, 82, 413 – 427.

570 Borghi, A., R. Compagnoni and M. Naldi (1996), The crystalline basement of the Canavese
571 Zone (Internal Western Alps): new data from the area west of Ivrea (Northern Italy), *Géol.*
572 *Alpine*, 72, 23–34.

573 Boriani, A., L. Burlini, V. Caironi, E. Giobbi Origoni, A. Sassi and E. Sesana (1988),
574 Geological and petrological studies on the Hercynian plutonism of Serie dei Laghi –

575 Geological Map of its occurrence between Valsesia and Lago Maggiore (N. Italy), *Rend.*
576 *Soc. It. Mineral. Petrol.*, 43, 367-384.

577 Boriani A. and R. Sacchi (1973), Geology of the junction between Ivrea Verbano and Strona
578 Ceneri Zones, *Mem Ist. Geol. Min. Univ. Padova*, 28, 36pp.

579 Boriani A. and I. Villa (1997), Geochronology of regional metamorphism in the Ivrea-
580 Verbano Zone and Serie dei Laghi, Italian Alps, *Schweiz. Mineral. Petrogr. Mitt.*, 77, 381-
581 401.

582 Boriani A. and E. Giobbi (2004), Does the basement of western southern Alps display a
583 tilted section through the continental crust? A review and discussion, *Per. Mineral.*, 73, 5-
584 22.

585 Casati, P. (1978), Tettonismo e sedimentazione nel settore occidentale delle Alpi
586 Meridionali durante il tardo Paleozoico, il Triassico e il Giurassico, *Riv. It. Paleont.*
587 *Stratigr.*, 84, 313-326.

588 Chenin, P., G. Manatschal, S. Picazo, O. Müntener, G. Karner, C. Johnson, and M. Ulrich
589 (2017), Influence of the architecture of magma-poor hyperextended rifted margins on
590 orogens produced by the closure of narrow versus wide oceans, *Geosphere*, 13(2), 559-
591 576, doi : <https://doi.org/10.1130/GES01363.1>

592 Chevalier, F., M. Guiraud, J.P. Garcia, J.L. Dommergues, D. Quesne and P. Allemand
593 (2003) Calculating the long- term displacement rates of a normal fault from the high-
594 resolution stratigraphic record (early Tethyan rifting, French Alps). *Terra Nova*, 15, 410-
595 416.

596 Costamagna, L.G. (2016) The Middle Jurassic Alpine Tethyan unconformity and the Eastern
597 Sardinia – Corsica Jurassic High: a sedimentary and regional analysis, *Journ. Iberian*
598 *Geology*, 42(3), 311-334.

599 Decandia, F.A. and Elter P. (1969) Riflessioni sul problema delle ofioliti nell’Appennino
600 settentrionale (nota preliminare), *Atti della Società Toscana di Scienze Naturali*, 76, 1-9.

601 Decarlis, A., G. Dallagiovanna, A. Lualdi, M. Maino and S. Seno (2013), Stratigraphic
602 evolution in the Ligurian Alps between Variscan heritages and the Alpine Tethys
603 opening: a review, *Earth Sci. Rev.*, 125, 43-68.

604 Decarlis, A., G. Manatschal, I. Hauptert and E. Masini (2015), The tectono-stratigraphic
605 evolution of distal, hyper-extended magma-poor conjugate rifted margins: Examples from
606 the Alpine Tethys and Newfoundland Iberia, *Marine and Petroleum Geology*, 68, 54-72.

607 De Graciansky, P. C., D. G. Roberts and P. Tricart (2011), The Western Alps, from rift to
608 passive margin to orogenic belt: an integrated geoscience overview, *Developments in*
609 *Earth Surface Processes*, 14, Elsevier: 397 pp, doi: [https://doi.org/10.1016/c2009-0-](https://doi.org/10.1016/c2009-0-64485-8)
610 64485-8

611 Doglioni, C. (1987), Tectonics of the Dolomites (Southern Alps, Northern Italy), *Journ.*
612 *Struct. Geol.*, 9, 181-193.

613 Elter, G., P. Elter, C. Sturani, and M. Weidmann (1966), Sur la prolongation du domaine
614 ligure de l’Apennin dans le Monferrat et les Alpes et sur l’origine de la Nappe de la
615 Simme s.l. des Préalpes romandes et chablaisiennes, *Arch. Sci. (Genève)*, 19, 279–377

616 Fantoni, R. and P. Scotti (2003), Thermal record of the Mesozoic extensional tectonics in
617 the Southern Alps, *Atti Ticin. Sci. Terra*, 9, 96–101.

618 Fantoni R., A. Decarlis and E. Fantoni (2003), Mesozoic extension at the western margin of
619 the Southern Alps (Northern Piedmont, Italy), *Atti Tic. Sc. Terra*, 44, 97-110.

620 Ferrando S., D. Bernoulli and R. Compagnoni (2004), The Canavese zone (internal Western
621 Alps): a distal margin of Adria, *Schweiz. Mineral. Petrogr. Mitt.*, 84, 237-256.

622 Froitzheim, N. and G. Manatschal (1996), Kinematics of Jurassic rifting, mantle
623 exhumation, and passive-margin in the Austroalpine and Penninic nappes (eastern
624 Switzerland), *Geol. Soc. of Am. Bull.*, 108, 1120–1133.

625 Gaetani, M. (2010), From Permian to Cretaceous: Adria as pivotal between extensions and
626 rotations of Tethys and Atlantic Oceans, in *The Geology of Italy: Tectonics and Life*
627 *Along Plate Margins*, J. Virtual Explor., vol. 36, edited by M. Beltrando et al., The Virtual
628 Explorer, Pty. Ltd., Clear Range, Australia, doi:10.3809/jvirtex.2010.00235.

629 Garutti, G., G. Rivalenti, A. Rossi and S. Sinigoi (1979), Mineral equilibria as geotectonic
630 indicators in the ultramafics and related rocks of the Ivrea-Verbano Basic Complex (Italian
631 Western Alps) Pyroxenes and Olivine, *Mem. Scienze Geologiche*, 33, 147–160.

632 Handy, M. R. (1987), The structure, age and kinematics of the Pogallo fault zone, southern
633 Alps, northwestern Italy. *Eclogae Geologicae Helvetiae*, 80, 593–632.

634 Handy, M. R., L. Franz, B. Heller, B. Janott and R. Zurbriegen (1999), Multistage accretion
635 and exhumation of the continental crust (Ivrea crustal section, Italy and Switzerland),
636 *Tectonics*, 18: 1154–1177.

637 Handy, M.R., S. M. Schmid, R. Bousquet, E. Kissling E. and D. Bernoulli (2010),
638 Reconciling plate-tectonic reconstructions of Alpine Tethys with the geological-
639 geophysical record of spreading and subduction in the Alps, *Earth Sci. Rev.*, 102, 121-158.

640 Hartmann, G. and K. H. Wedepohl (1993), The composition of peridotite tectonites from the
641 Ivrea Complex, northern Italy: residues from melt extraction, *Geochemica et*
642 *Cosmochimica Acta*, 57, 1761–1782.

643 Hauptert, I., G. Manatschal, A. Decarlis and P. Unternehr (2016), Upper-plate magma-poor
644 rifted margins: Stratigraphic architecture and structural evolution, *Marine and Petroleum*
645 *Geology*, 69, p. 241-261.

646 Kalin, O. and Trümpy D. (1977) Sedimentation und Palaotektonik in den westlichen
647 Sudalpen: zur triassisch-jurassischen Geschichte des Monte Nudo-Beckens. *Eclogae*
648 *Geologicae Helvetiae*, 70, 295-305.

649 Lavier, L. and G. Manatschal (2006), A mechanism to thin the continental lithosphere at
650 magma-poor margins, *Nature*, 440, 324–328.

651 Lemoine M., Tricart P., and Boillot G. (1987) Ultramafic and gabbroic ocean floor of the
652 Ligurian Tethys (Alps, Corsica, Apennines): In search for a genetic model, *Geology*, 15,
653 622-625.

654 Lemoine, M., T. Bas, A. Arnaud-Vanneau, H. Arnaud, T. Dumont, M. Gidon, P. C. De
655 Graciansky, J. L. Rudkiewicz, J. Megard-Galli J. and P. Tricart (1986), The continental
656 margin of the Mesozoic Tethys in the Western Alps, *Mar. Petrol. Geol.*, 3, 179-199.

657 Lister, G. S. and G. A. Davies (1989), The origin of metamorphic core complexes and
658 detachment faults formed during the Tertiary continental extension in northern Colorado
659 River region, U.S.A., *Journ. Struct. Geol.*, 11(1/2), 65-94.

660 Lister, G., M.A. Etheridge and P.A. Symonds (1986), Detachment faulting and the evolution
661 of passive continental margins, *Geology*, 14, 246-250.

662 Manatschal, G. (1999), Fluid- and reaction-assisted low angle normal faulting: evidence
663 from rift-related brittle fault rocks in the Alps (Err Nappe, eastern Switzerland), *J. Struct.*

664 *Geol.*, 21(7), 777-793.

665 Manatschal, G. (2004), New models for evolution of magma-poor rifted margins based on a
666 review of data and concepts from West Iberia and the Alps, *Int. Jour. of Earth Sci.*, 93,
667 432–466.

668 Manatschal, G., A. Engström, L. Desmurs, U. Schaltegger, M. Cosca, O. Müntener and D.
669 Bernoulli (2006), What is the tectono-metamorphic evolution of continental break-up: the
670 example of the Tasma Ocean-Continent transition, *J. Struct. Geol.*, 28, 1849–1869.

671 Manatschal, G. and D. Bernoulli (1999), Architecture and tectonic evolution of non-volcanic
672 margins: present-day Galicia and ancient Adria, *Tectonics*, 18(6), 1099-1199.

673 Masini, E., G. Manatschal, G. Mohn, J-F Ghienne and F. Lafont (2011), The tectono-
674 sedimentary evolution of a supradetachment rift basin at a deep water magma-poor rifted
675 margin: the example of the Samedan Basin preserved in the Err nappe in SE Switzerland,
676 *Basin Res.*, 23, 652-677.

677 Masini, E., G. Manatschal and G. Mohn (2013), The Alpine Tethys rifted margins:
678 reconciling old and new ideas to understand the stratigraphic architecture of magma-poor
679 rifted margins, *Sedimentology*, 60, 174-196.

680 Mohn, G., G. Manatschal, M. Beltrando, E. Masini and N. Kusznir (2012), Necking of
681 continental crust in magma-poor rifted margins: Evidence from the fossil Alpine Tethys
682 margins, *Tectonics*, 31, doi:10.1029/2011TC002961.

683 Mohn, G., G. Manatschal, Othmar Müntener, M. Beltrando and E. Masini (2010)
684 Unravelling the interaction between tectonic and sedimentary processes during lithospheric
685 thinning in the Alpine Tethys margins, *International Journal of Earth Science*, 99(1), 75-
686 101, doi: 10.1007/s00531-010-0566-6.

687 Montanari, L. (1969), Aspetti geologici del Lias di Gozzano (Lago d'Orta), *Mem. Soc. It. Sc.*
688 *Nat. Mus. Civico Storia Nat. Milano*, 18, 25-94.

689 Muttoni, G., D. V. Kent, E. Garzanti, P. Brack, N. Abrahamsen and M. Gaetani (2003),
690 Permian Pangea "B" to Late Permian Pangea "A", *Earth and Pl. Sc. Letters*, 215, 379-394.

691 Novarese, V. (1929), La Zona del Canavese e le formazioni adiacenti, *Mem. Descrittive*
692 *della Carta Geologia d'Italia*, 22, 65–212.

693 Peron-Pinvidic, G., G. Manatschal, E. Masini, E. Sutra, J. M. Flament, I. Hauptert and P.
694 Unternehr (2017), Unraveling the along-strike variability of the Angola-Gabon rifted
695 margin: a mapping approach, in *Petroleum Geoscience of the West Africa Margin* edited
696 by Sabato, C. T., R. A. Hodgkinson and G. Backe, *Geol. Soc. London*, SP 438,
697 <http://doi.org/10.1144/SP438.1>.

698 Pfiffner, A. (2016), Basement-involved thin-skinned and thick-skinned tectonics in the Alps,
699 *Geol. Mag.*, 153, 1085-1109.

700 Pfiffner, A. (2014), *Geology of the Alps*, Wiley-Blackwell, 368 pp. ISBN: 978-1-118-
701 70813-5.

702 Pinarelli, L., A. Boriani and A. Del Moro (1988), Rb-Sr geochronology of the Lower
703 Permian plutonism in Massiccio dei Laghi, Southern Alps (NW Italy), *Rend. Soc. It.*
704 *Mineral. Petrol.*, 43, 411-428.

705 Rivalenti G., G. Garuti, A. Rossi, F. Siena and S. Sinigoi (1981), Existence of different
706 peridotite types and of a layered igneous complex in the Ivrea Zone of the western Alps,
707 *Journal of Petrology*, 22, 127–153.

708 Sacchi Vialli, G. and G. M. Cantaluppi (1967), I nuovi fossili di Gozzano, *Mem. Soc. It. Sc.*
709 *Nat. Milano*, 16, 238-296.

710 Sbisà, A. (2010), Structure and eruptive history of the Sesia caldera (Northwest Italy),
711 *Unpublished PhD Thesis, Università degli Studi di Trieste*, 140 pp. Download at:
712 <https://www.openstarts.units.it/dspace/handle/10077/4560>

713 Siegesmund, S., P. Layer, I. Dunkl, A. Vollbrecht, A. Steenken, K. Wemmer and H.
714 Ahrendt (2008), Exhumation and deformation history of the lower crustal section of the
715 Valstrona di Omegna in the Ivrea Zone, Southern Alps, *Geol. Soc. London*, S.P. 298, 45-
716 68.

717 Schmid, S. M., H. R. Aebli, F. Heller and A. Zingg (1989), The role of the Periadriatic line
718 in the tectonic evolution of the Alps, *Geol. Soc. London*, S.P., 45, 151-171.

719 Schmid, S. M., Zing A., Handy M. (1987) The kinematics of movements along the Insubric
720 line and the emplacement of the Ivrea Zone. *Tectonophysics*, 135, 47-66.

721 Schmid, S. M., B. Fügenschuh, E. Kissling and R. Schuster (2004), Tectonic map and
722 overall architecture of the Alpine orogen, *Eclog. Geol. Helv.*, 97, 93-117.

723 Schumacher M. E. (1997), Geological interpretation of the seismic profiles through the
724 Southern Alps (lines S1-S7 and C3 South), in: Pfiffner et al., *Deep Structure of the Swiss*
725 *Alps Results from NRP 20*, Birkhäuser, Basel, 101-114

726 Shervais, J. (1979), Ultramafic and mafic layers in the Alpine-type Lherzolite massif at
727 Balmuccia (NW Italy), *Mem. Scienze Geologiche*, 33, 135-145.

728 Sutra, E. , G. Manatschal, G. Mohn and P. Unternehr (2013), Quantification and restoration
729 of extensional deformation along the Western Iberia and Newfoundland rifted margins,
730 *Geoch., Geoph., Geosys*, 14 (8), 2575-2597.

731 Stampfli, G. M., G. D. Borel, R. Marchant and J. Mosar (2002), Western Alps geological
732 constraints on western Tethyan reconstructions, in Reconstruction of the Evolution of the
733 Alpine-Himalayan Orogen edited by Rosenbaum, G. and G. S. Lister, *Journ. Virtual Expl.*,
734 7, 75-104.

735 Sturani, C. (1973), Considerazioni sui rapporti tra Appennino settentrionale ed Alpi
736 occidentali. In: Moderne vedute sulla geologia dell'Appennino. *Quaderni dell'Accademia*
737 *Nazionale dei Lincei*, 183, 119–142.

738 Sturani, C. (1964), Prima segnalazione di Ammoniti nel Lias del Canavese, *Rend. Accad.*
739 *Lincei*, 37, 482–483.

740 Tugend, J., G. Manatschal, Kuszniir N. and E. Masini (2014), Characterizing and identifying
741 structural domains at rifted continental margins: application to the Bay of Biscay margins
742 and its Western Pyrenean fossil remnants, *Geol. Soc. of London*, S. P. 413.

743 Thierry, J. et al. (44 co-authors) (2000a): Map 10: Early Kimmeridgian (146-144 Ma): In:
744 Dercourt, J., Gaetani, M., Vrielyneck, B., Barrier, E., Biju-Duval, B., Brunet, M.F., Cadet,
745 J.P., Crasquin, S. & Sandulescu, M. (Eds.), Atlas Peri-Tethys, Paris, palaeogeographical
746 map.

747 Thierry, J. et al. (42 co-authors) (2000b) Map 11: Early Tithonian (141-139 Ma): In:
748 Dercourt, J., Gaetani, M., Vrielyneck, B., Barrier, E., Biju-Duval, B., Brunet, M.F., Cadet,
749 J.P., Crasquin, S. & Sandulescu, M. (Eds.), Atlas Peri-Tethys, Paris, palaeogeographical
750 map.

751 Turrini, C., O. Lacombe and F. Roure (2014), Present-day 3D structural model of the Po
752 Valley basin, Northern Italy, *Mar. Petrol. Geol.*, 56, 266–289,
753 doi:10.1016/j.marpetgeo.2014.02.006.

754 Voshage, H., S. Sinigoi, M. G. Mazzucchelli, G. Rivalenti and A. W. Hofmann (1988),
755 Isotopic constraints on the origin of ultramafic and mafic dikes in the Balmuccia peridotite
756 (Ivrea Zone), *Contributions to Mineralogy and Petrology*, 100, 261–267.

757 Wozniak, J. (1977), Contribution à l'Étude des Alpes occidentales internes. La région du
758 Canavese (Italie), Thesis, Univ. Pierre et Marie Curie, Paris.

759 Zanetti, A., M. Mazzucchelli, S. Sinigoi, T. Giovanardi, G. Peressini, M. Fanning (2013),
760 SHRIMP U-Pb zircon Triassic intrusion age of the Finero Mafic Complex (Ivrea-Verbano
761 Zone, Western Alps) and its geodynamic implications, *Journal of Petrology*, 54, 2235-
762 2265.

763 Zingg, A. (1990), The Ivrea crustal cross-section (Northern Italy and Southern Switzerland),
764 in Exposed cross section of the continental crust, edited by Salisbury, M. H. and M.
765 Fountain, Kluwer Academic publisher, Dordrecht, 1-21.

766 Zanin Buri C. (1965), Il Trias in Lombardia (studi geologici e paleontologici). XIII. Le
767 alghe calcaree delle Prealpi Lombarde, *Riv. It. Paleont. Stratigr.* 71(2), 449-544.

768 Zingg, A., M. R. Handy, J. Hunziker and S.M. Schmid (1990), Tectonometamorphic
769 history of the Ivrea Zone and its relationship to the crustal evolution of the southern Alps,
770 *Tectonophysics*, 182, 169–192.

771

772 **Captions**

773 Fig. 1: (a): Location and (b) structural map of the Western-Central Alps [from Schmid
774 et al., 2004, mod.]. Yellow frame indicates the study area. (c): Simplified
775 palaeogeographic setting of the Alpine domain during Late Jurassic, showing the
776 main plates involved in the Ligurian-Piedmont rifting. (d): Cross section across
777 the Alpine Tethys illustrating the main Alpine palaeogeographic structural
778 domains and rifting domains; OCT: ocean-continent transition zone [from
779 Decarlis et al., 2015].

780 Fig. 2: Conceptual kinematic model for magma-poor rifted margin evolution in time
781 [from *Hauptert et al.*, 2016] from pre-rift (a) to breakup stage (d). Details of the
782 evolutionary stages and nomenclature description in the text. Note the formation
783 of the “H-block” [*Lavier and Manatschal*, 2006] and its uplift at the beginning
784 of thinning phase (b) before being drowned after the onset of the main
785 detachment fault. Then it lies dissected (“residual H Block”: $H_{(r)}$) at one side of
786 the system as a major indicator for upper plate geometry (c; see also Fig 3); Φ :
787 Necking faults; ϕ : R2 fault; Ψ : Main detachment fault; A-B: reference points for
788 extension rate. Vertical exaggeration: 1.6.

789 Fig. 3: (a-b): Interpretative sections across the Alpine conjugate margins of Europe and
790 Northern Adria during Syn-tectonic sequence 1 and sequence 2 deposition (STS₁
791 and STS₂) [*Decarlis et al.*, 2015]. (c): Toarcian; logarithmic vertical scale); from
792 *Decarlis et al.* [2015]. (d): Conceptual basin-types developing along an idealized
793 rifted margins section [from *Decarlis et al.*, 2015]: 1 Half-graben basin of the
794 proximal margin with STS₂ progressively sealing the topography; 2 Uplifted
795 sector of the distal margin almost completely lacking the whole syn-tectonic
796 succession; 3 Drowned sector of the distal margin characterized by the thick
797 clastic STS₂; 4 Supra-detachment basin, characterized by the occurrence of

798 exhumed basement/mantle and continental derived clast. Note the allochthonous
799 block on the right. (see text). (e): Key features of the STS1 and STS2
800 sedimentation along rifted margin section.

801 Fig. 4: (a-b): Location and simplified geological-structural map of the study area [from
802 *Siegesmund et al.*, 2008; *Schumacher*, 1997; modified]. Key location cited in the
803 text: In: Inverio; Gz: Gozzano; Mf: Monte Fenera; So: Sostegno; Md: Montalto
804 Dora; Le: Levone. Main Structural lines: I.L.: Insubric Line s.l.; C.M.B.: Cossato-
805 Mergozzo-Brissago Line; P.L.: Pogallo Line; C.L.: Cremosina Line; E.C.L.:
806 External Canavese Line; I.C.L.: Internal Canavese Line. Additional elements of the
807 Southalpine domain: Nb: Monte Nudo basin; Gb: Monte Generoso basin. (c)
808 Stratigraphic scheme of the sedimentary cover of the Southern Alps [from
809 *Beltrando et al.*, 2015a]. Red boxes indicate the two main Jurassic phases of the
810 Alpine rifting respectively acting in the proximal (Lombardian basin) and distal
811 margin (Cusio-Biellese-Canavese). References for the stratigraphy of the different
812 sectors: (1) *Elter et al.* [1966], (2) *Beltrando et al.* [2015a], (3) *Ferrando et al.*,
813 [2004], (4) *Sturani* [1964], (5) *Berra et al.* [2009], (6) *Casati* [1978], (7) *Montanari*
814 [1969], (8) *Bertotti et al.* [1993], (9) *Berra et al.* [2009], and (10) *Berra and*
815 *Carminati* [2010].

816 Fig. 5: Stratigraphic sections of the main western Southalpine outcrops west of Lago
817 Maggiore, drawn on the base of the cited literature and of personal field
818 observations. For locations see Fig. 4. See text for detailed description. Relevant
819 GPS points are indicated in Lat/Long decimal degrees. Please note the different
820 scales.

821 Fig 6: (a): Monogenic breccia with cm to dm clasts of Triassic dolostones and sparse

822 fragments of reddish pelite (palaeosol?); Arona. **(b)**: Polygenic breccia with
823 dolostone (dls), basement (bs) and riolyte (ri) clasts; Inverio. **(c)**: Reddish
824 calcarenite of Lithozone A, with widespread evidences for diffused fluid
825 circulation; Gozzano. **(d)**: Interpretative sketch from *Montanari* [1969] of the
826 angular unconformity between U. Sinemurian - L. Pliensbachian (Lithozone A) and
827 U. Pliensbachian (Lithozone B) deposits; Gozzano. **(e)**: Microconglomerate with
828 dolomitic clasts at the top of the Triassic dolostones at Monte Fenera, interpreted as
829 a reworked Jurassic paleosol deposited in a shallow water basin **(f)** Sedimentary
830 dikes with reddish pelites infill and dolomitic breccia inside the Ladinian
831 dolostones at Sostegno. Breccia derives from the karstification of the top of the
832 Ladinian platform. White clasts ranging from sub-cm to dm in size are formed by
833 dolostone. **(g)**: Tectonostratigraphic breccia found at Bric Filia (Canavese Zone)
834 locally directly overlying the lower crust migmatites (not in photo). Clasts and
835 matrix are formed by differently sized debris of lower crust substratum. Only at the
836 top sparse dolomitic clasts occur. **(h)**: Middle Jurassic siliceous schists associated
837 to the Radiolarite Formation near Bric Filia (Canavese Zone).

838 Fig. 7 (a) Simplified reconstruction of the Adriatic margin during the Middle Jurassic
839 from Lombardy basin to the Canavese Zone, from *Beltrando et al.* [2015], mod. For
840 locations see Fig. 4. (b) Conceptual 3D model of the distal sector of the Southern
841 Adria margin. See text for detailed explanation. Locations and fault abbreviations
842 as in Fig. 4. **(b)**: Same view with the “H-Block” (T2) exploded to highlight the
843 complex fault bounded structure and the suggested relationships with the
844 outcropping faults. Pogallo Line (PL) may represent at the surface either the lower
845 necking system or the coupling line Note that Cossato Mergozzo Brissago Line
846 (CMB) do not necessary correspond to the Jurassic Upper-Lower crustal boundary

847 over all the section, as it represents an inherited line.

848 Fig. 8 **(a-b)**: Location and interpretative map of the Alps where major tectonic units are
849 mapped as rifting domain [*Hauptert et al.*, 2016]. **(c)**: Schematic interpretative
850 sections through the Upper plates sections of Southern Adria (A-A1: see text in this
851 paper) and Europe-Northern Adria rifted margins (B-B1) [*Decarlis et al.*, 2015].
852 **(d)**: Paleogeographic reconstruction of the Western Mediterranean during Late
853 Jurassic. The proposed distribution of different upper plates and lower plates in the
854 Alpine domains suggests the existence of a major “transfer” fault cutting apart
855 Southern from Northern Adria and possibly Europe from Iberia.

Figure 1.

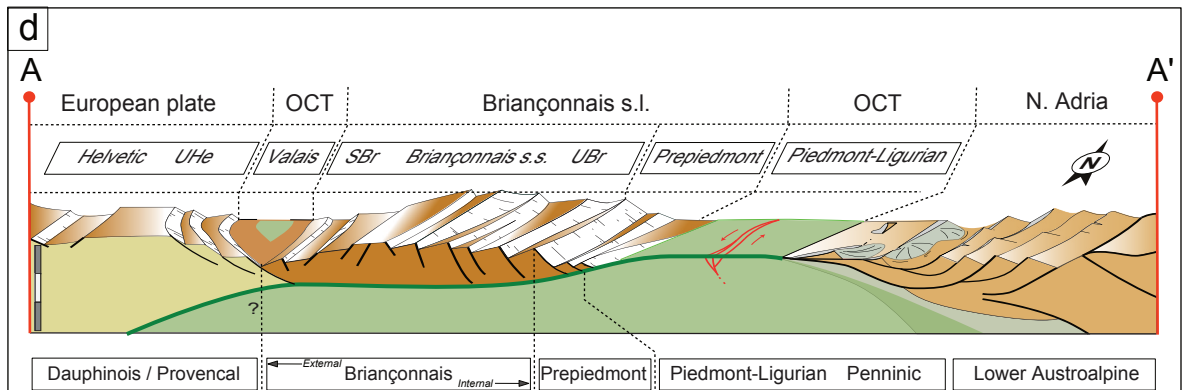
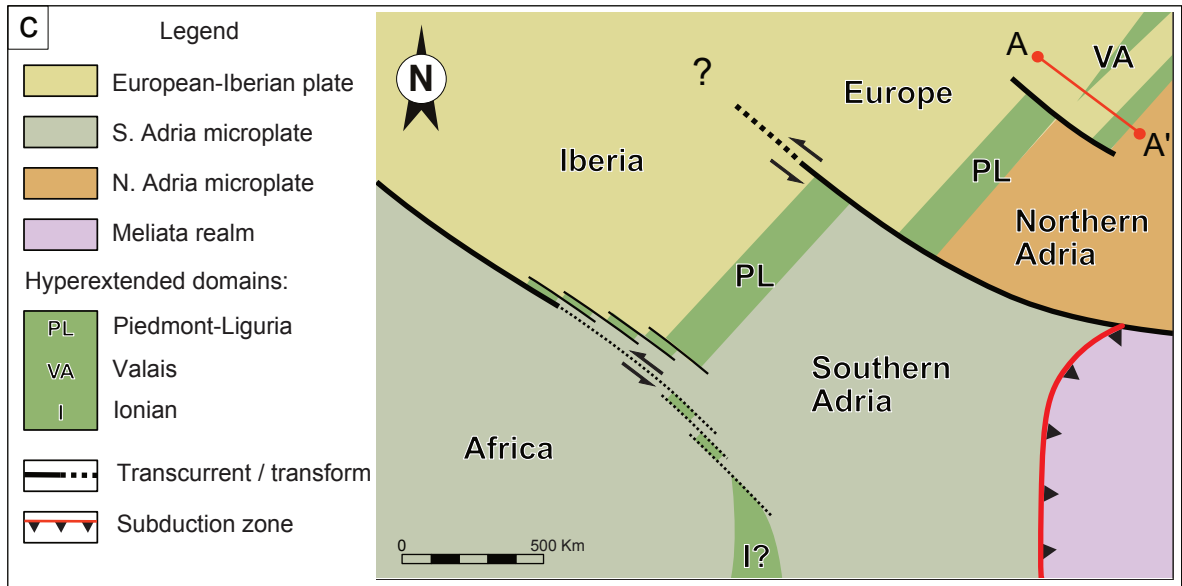
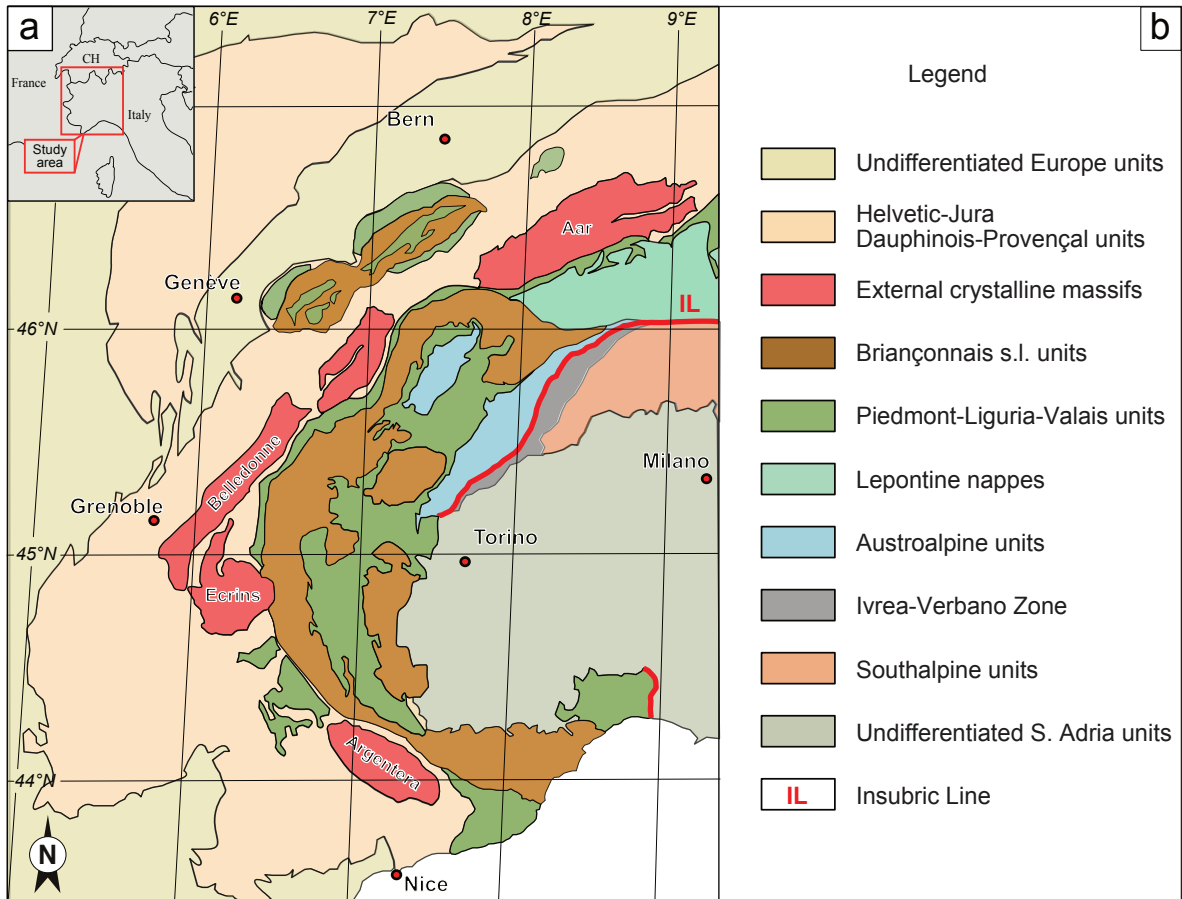


Figure 2.

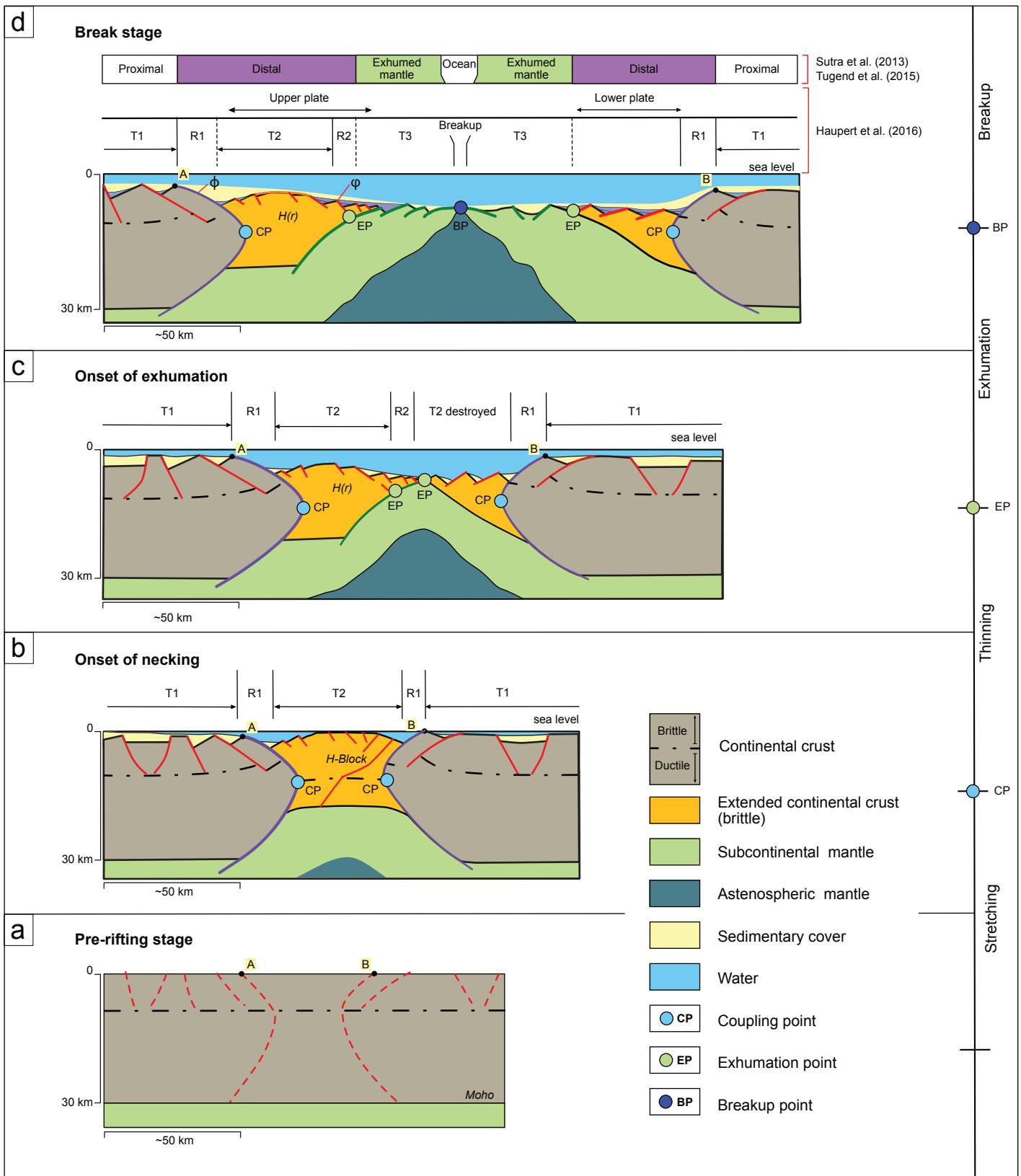


Figure 3.

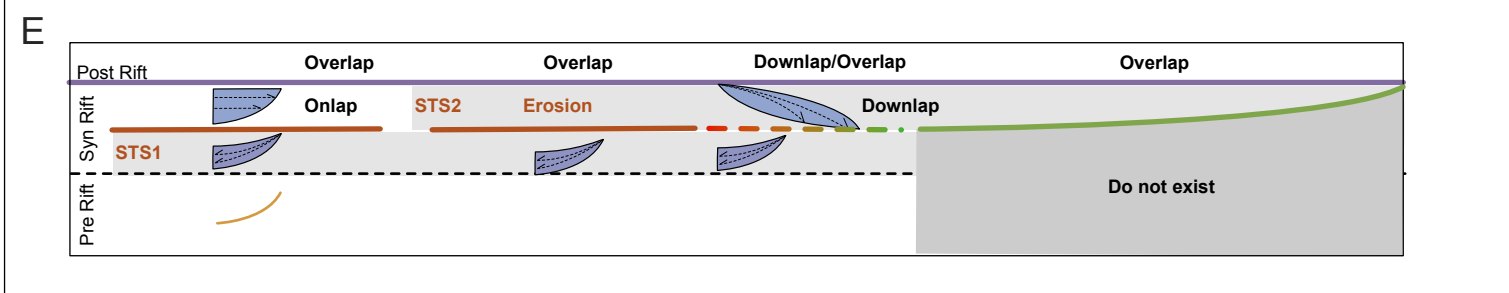
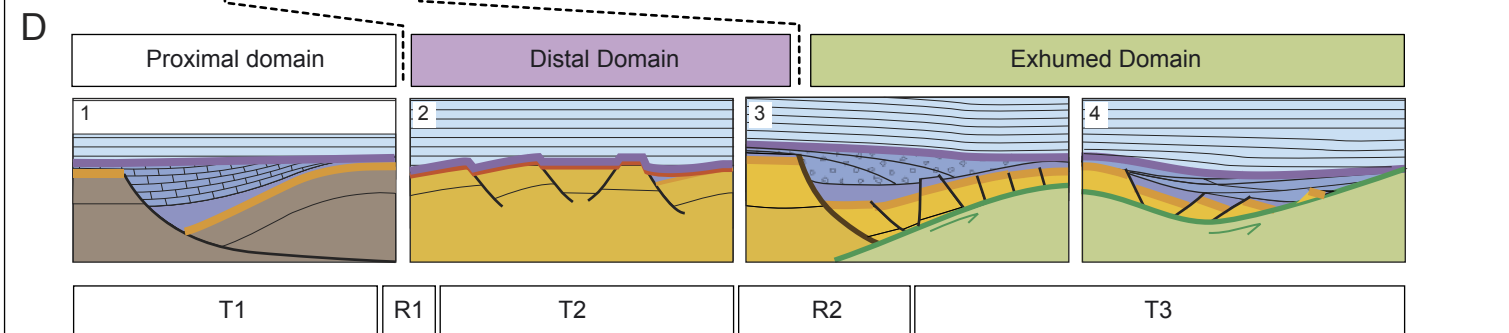
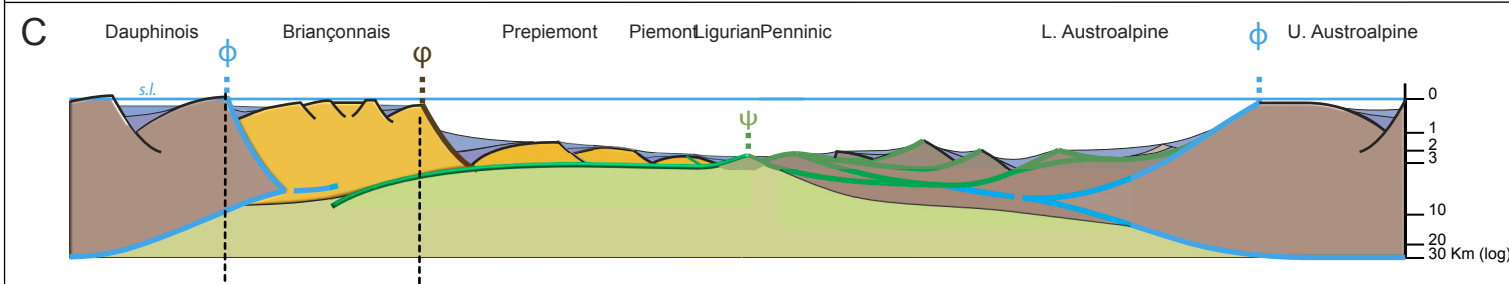
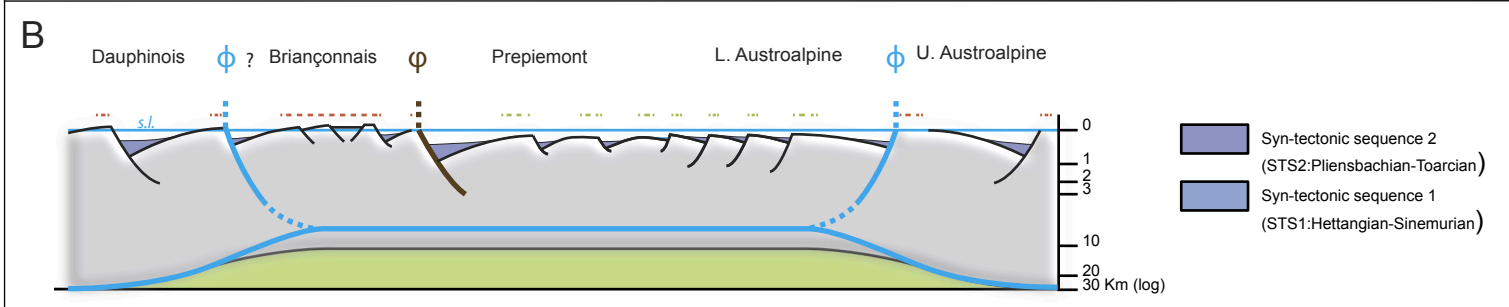
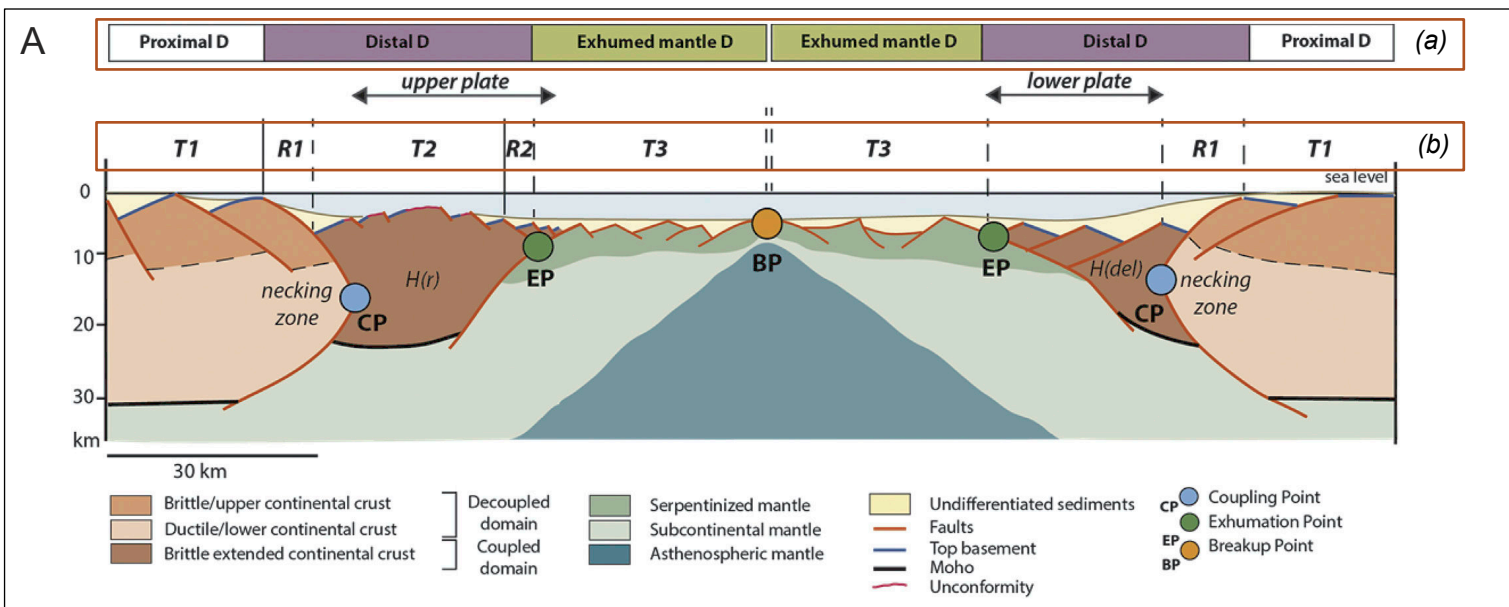


Figure 4.

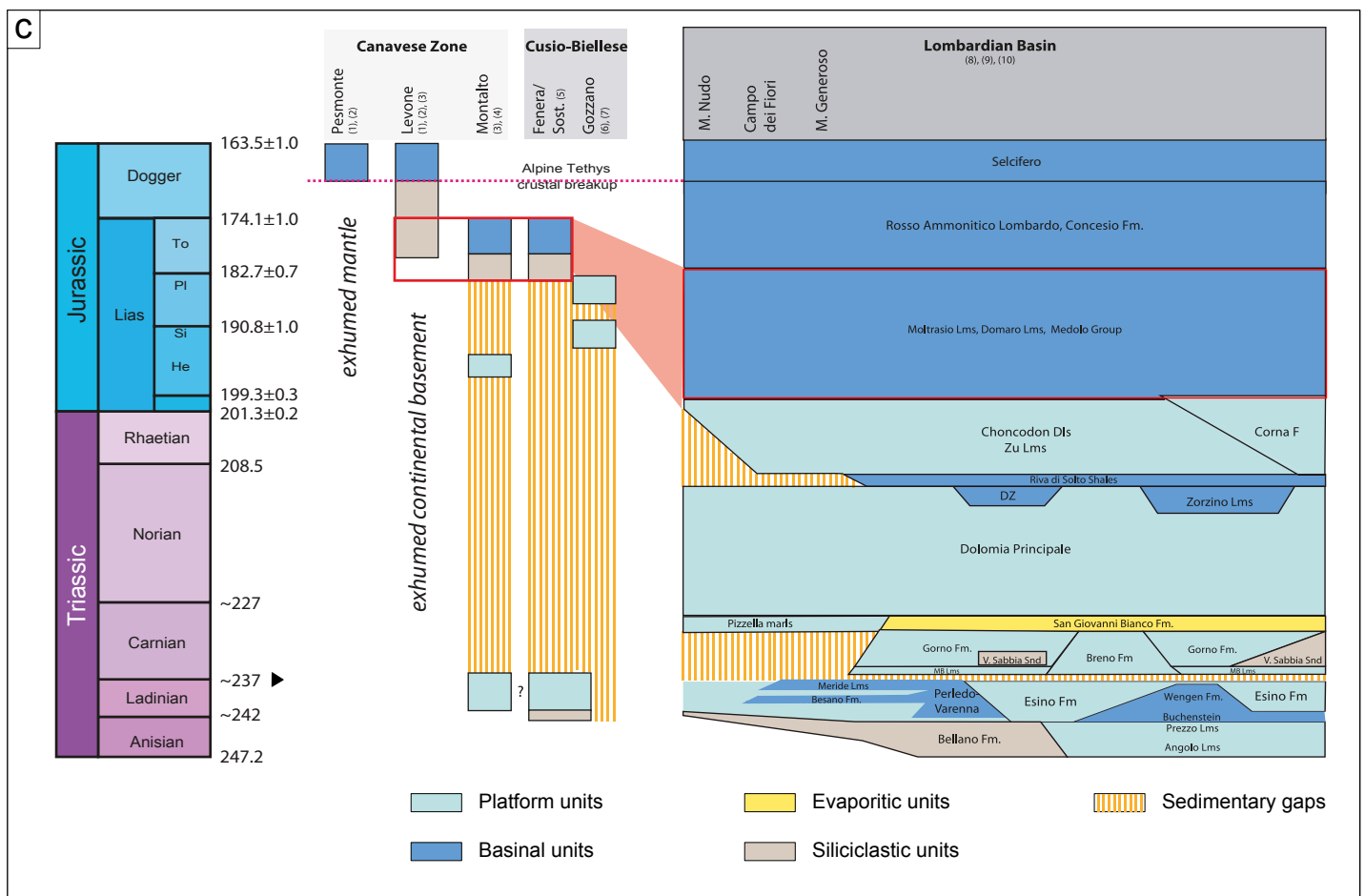
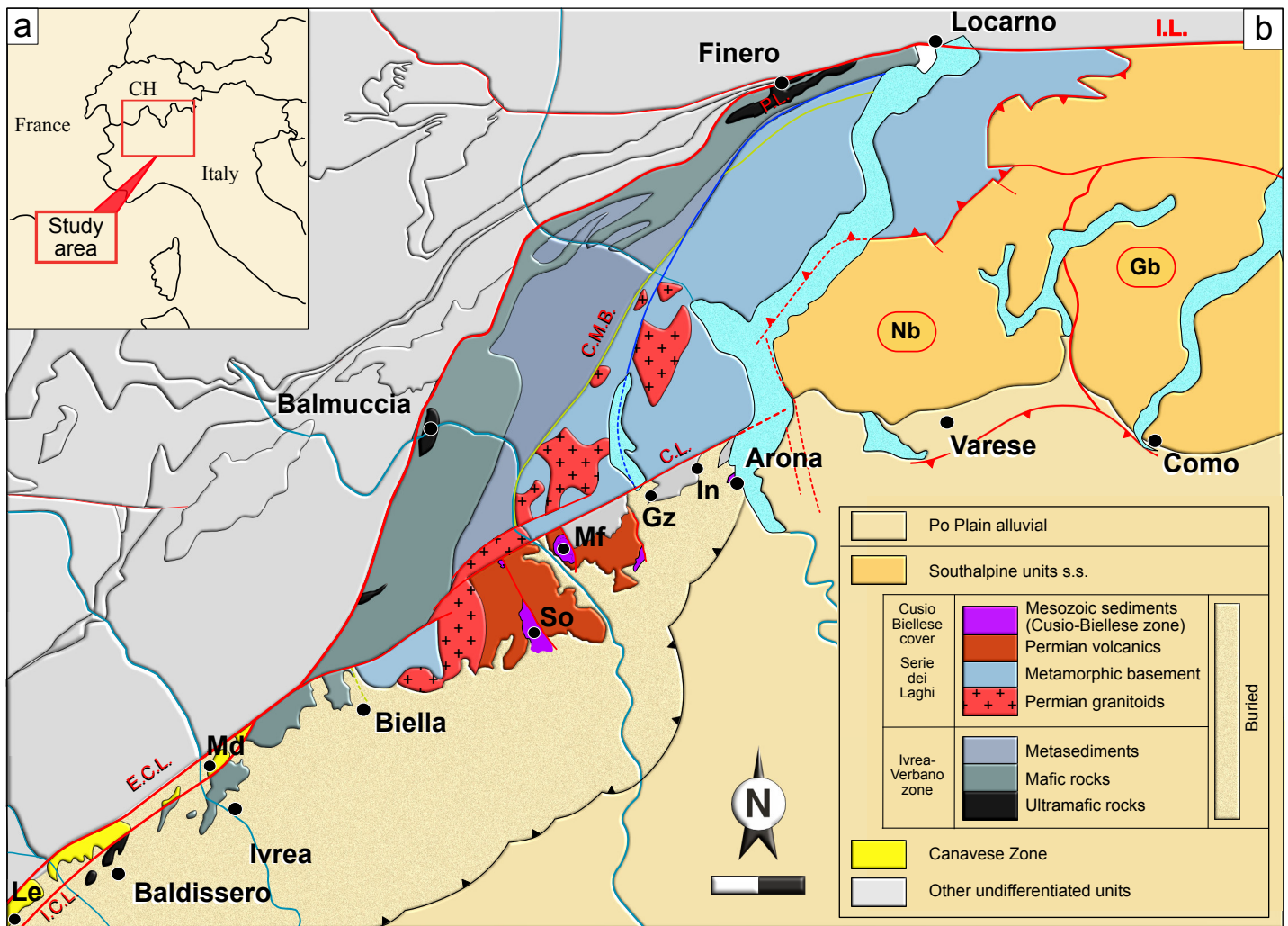


Figure 5.

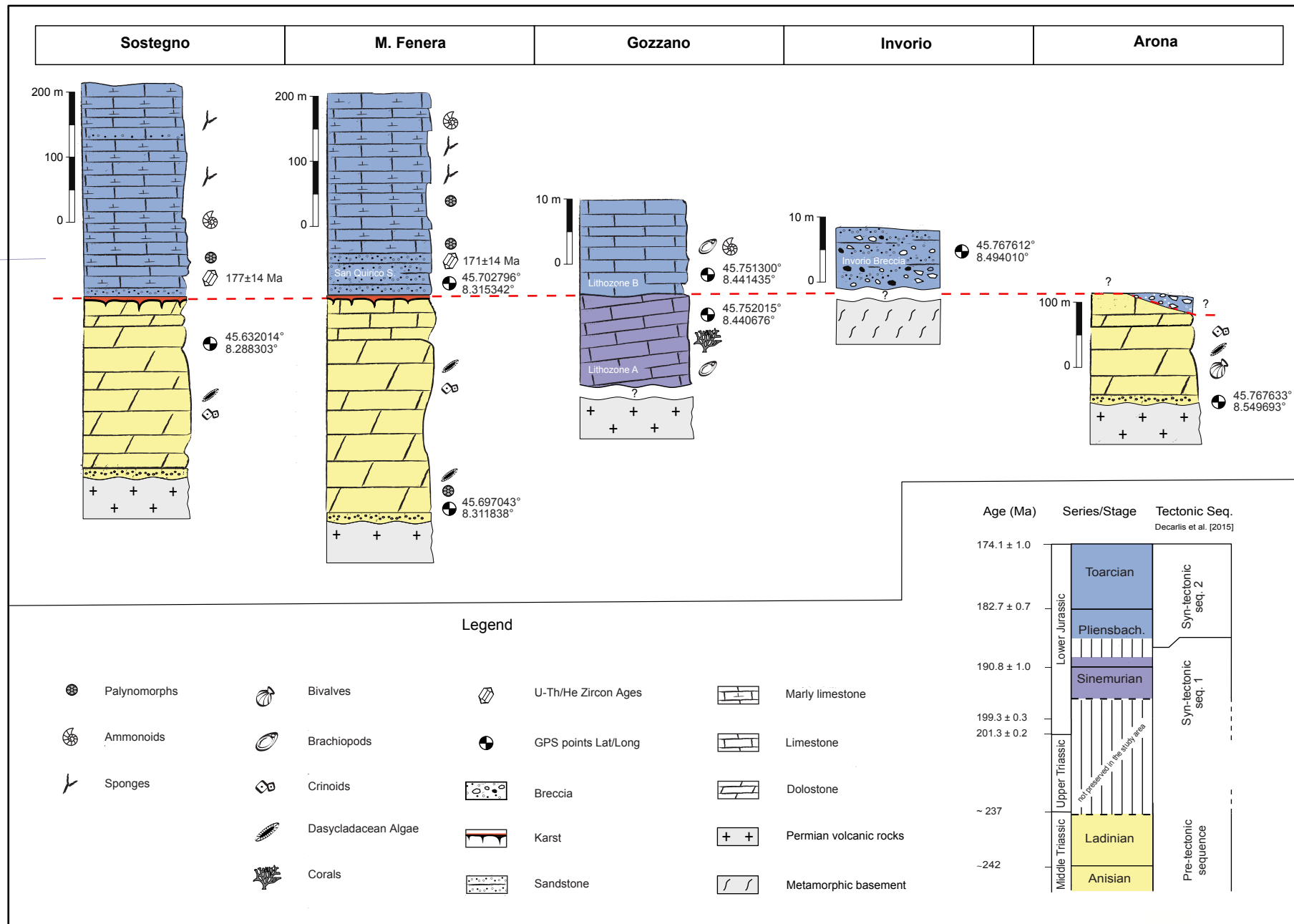


Figure 6.

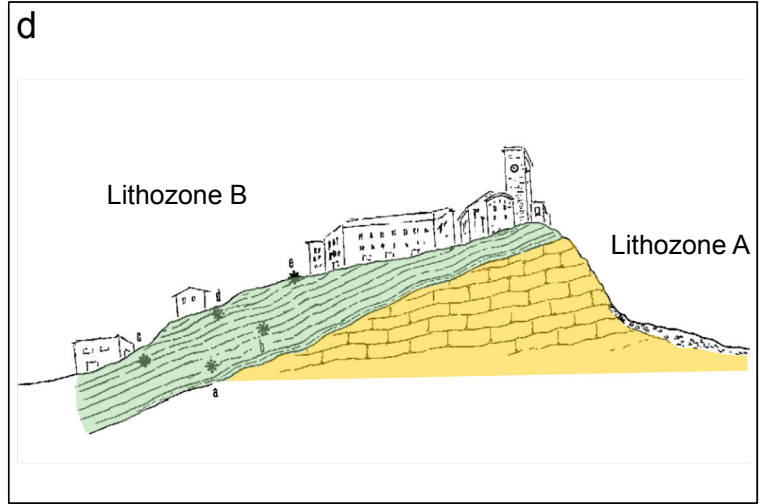
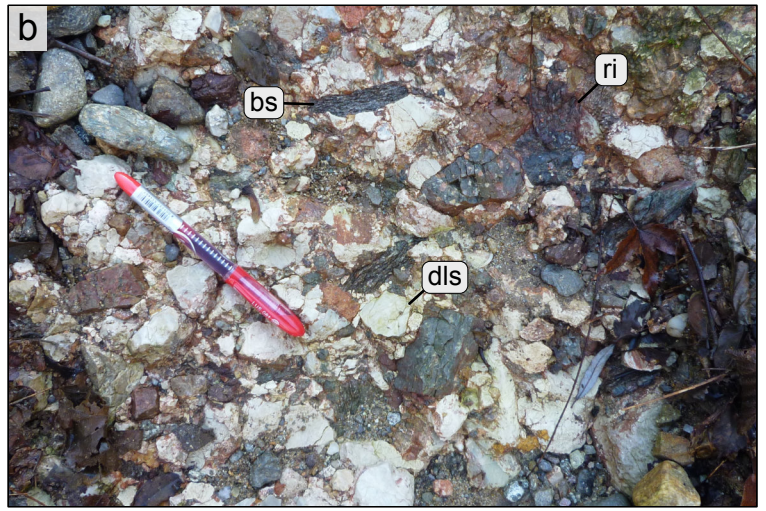


Figure 7.

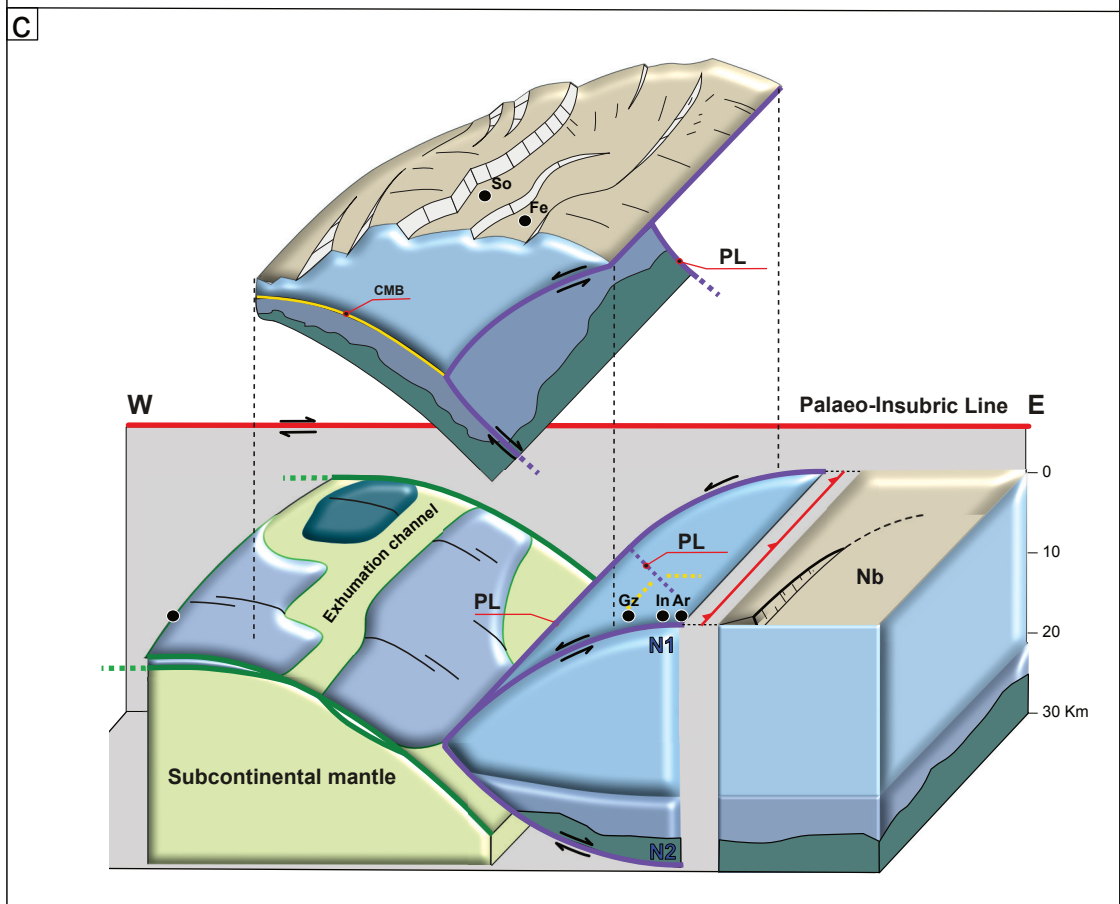
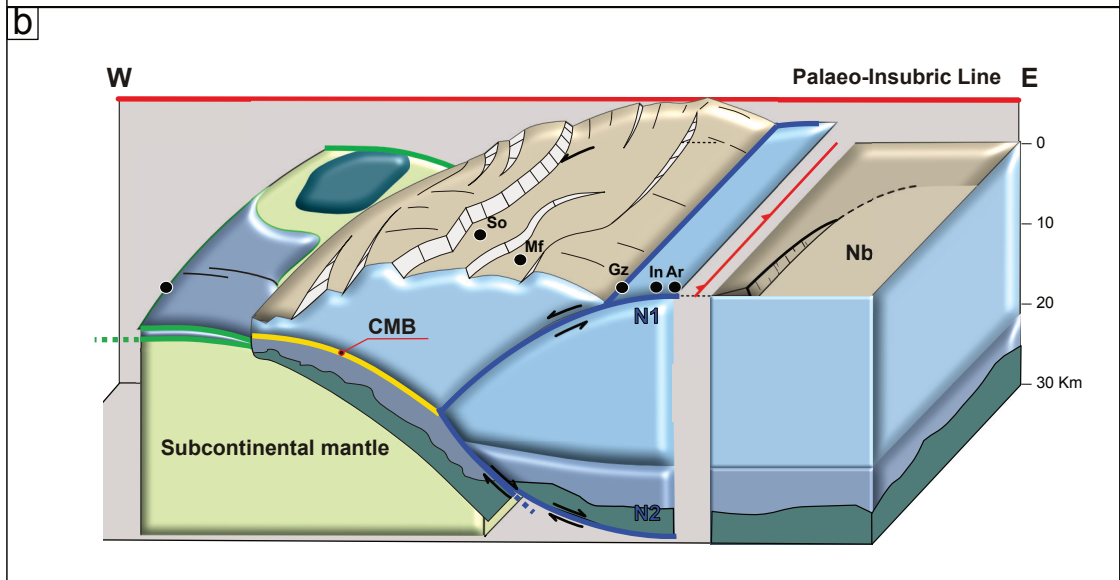
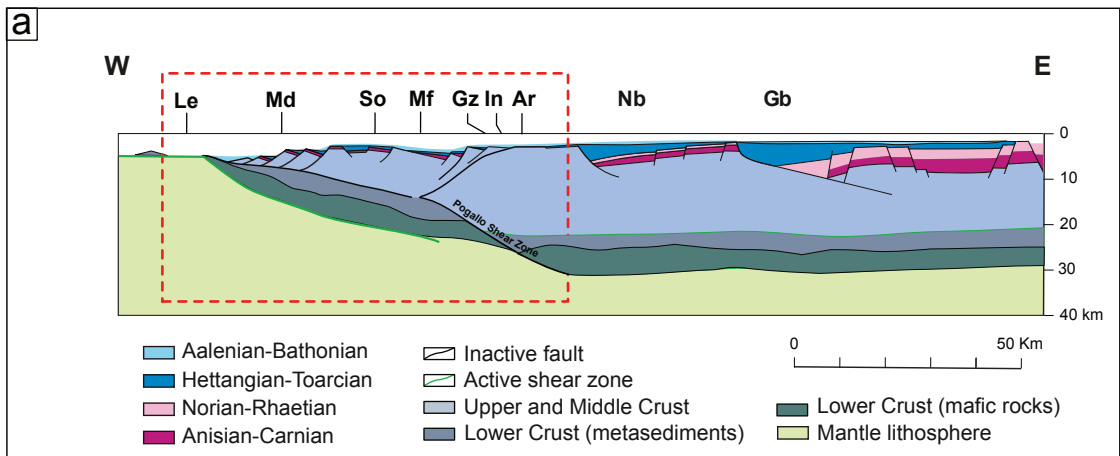


Figure 8.

